Published in final edited form as:
Mech Dev. 2013 February ; 130(2-3): 143–159. doi:10.1016/j.mod.2012.09.010.

Conditional deletions refine the embryonic requirement for *Dlk1*

Oliver K. Appelbe[a], **Aleksey Yevtodiyenko**[a,b], **Hilmarie Muniz-Talavera**[a], and **Jennifer V. Schmidt**[a]

Oliver K. Appelbe: oappel2@uic.edu; Aleksey Yevtodiyenko: ayevto1@stanford.edu; Hilmarie Muniz-Talavera: munizta1@uic.edu; Jennifer V. Schmidt: jvs@uic.edu

[a]Department of Biological Sciences, University of Illinois at Chicago, 900 S. Ashland Avenue, Chicago, IL 60607 USA

Abstract

Numerous studies have implicated Delta-like 1 (DLK1), a transmembrane protein that shares homology with Notch ligands, in embryonic growth and differentiation. *Dlk1* expression is widespread, though not ubiquitous, during early development, but is confined to a few specific cell types in adults. Adult *Dlk1*-expressing tissues include the Insulin-producing β-cells of the pancreas and the Growth hormone-producing somatotrophs of the pituitary gland. Previously generated *Dlk1* null mice ($Dlk1^{Sul\text{-}pat}$), display a partially penetrant neonatal lethality and a complex pattern of developmental and adult phenotypes. Here we describe the generation of a conditional *Dlk1* mouse line ($Dlk1^{flox}$) to facilitate cell type-specific deletion of the *Dlk1* gene, providing a powerful system to explore each aspect of the *Dlk1* null phenotype. Four tissue-specific Cre mouse lines were used to produce individual *Dlk1* deletions in pancreatic β-cells, pituitary somatotrophs and the endothelial cells of the embryo and placenta, key candidates for the *Dlk1* phenotype. Contrary to expectations, all of these conditional mice were fully viable, and none recapitulated any aspect of the $Dlk1^{Sul\text{-}pat}$ null mice. *Dlk1* expression is therefore not essential for the normal development of β-cells, somatotrophs and endothelial cells, and the tissues responsible for the *Dlk1* null phenotype remain to be identified. $Dlk1^{flox}$ mice will continue to provide an important tool for further research into the function of *Dlk1*.

Keywords

Dlk1; conditional knockout; pancreas; pituitary; endothelial cell

1. INTRODUCTION

1.1 Dlk1 is an imprinted transmembrane signaling molecule

Delta-like 1 (DLK1), also known as preadipocyte factor 1 (PREF-1), is a single-pass transmembrane protein containing EGF-like repeats homologous to the Notch ligands Delta, Jagged and Serrate (Smas and Sul, 1993). Unlike these ligands, however, DLK1 lacks a Notch interaction domain and may act as a repressor of Notch signaling (Ross et al., 2004). Full-length DLK1 is cleaved in the juxtamembrane region by tumor necrosis factor α

Address Correspondence to: Jennifer V. Schmidt, Ph.D. University of Illinois at Chicago, Department of Biological Sciences, 900 S. Ashland Avenue MC 567, Chicago, IL 60607 USA, Phone: 312-996-5655, Fax: 312-413-2691, jvs@uic.edu.
[b]Present address: Stanford University, Stanford CA

converting enzyme (TACE; ADAM17) to generate a soluble form of the protein that is referred to as fetal antigen 1 (FA1) (Bachmann et al., 1996; Smas et al., 1997; Wang and Sul, 2006). DLK1 has been implicated in multiple developmental processes including the differentiation of neuroendocrine cells and hepatocytes, hematopoiesis, osteogenesis and adipogenesis (Bauer et al., 1998; Floridon et al., 2000; Kaneta et al., 2000; Moore et al., 1997; Ohno et al., 2001; Tanimizu et al., 2003) (Abdallah et al., 2004; Garces et al., 1999; Lee et al., 2003; Li et al., 2005; Sakajiri et al., 2005; Smas and Sul, 1993). Overall, DLK1 appears to function in numerous cell types to regulate the switch from immature proliferating cells to a mature differentiated state.

Dlk1 is subject to genomic imprinting with expression only from the paternally inherited allele, while the maternally inherited allele remains silent (Kobayashi et al., 2000; Schmidt et al., 2000; Takada et al., 2000). In the mouse, *Dlk1* expression is first observed at embryonic day 11 (e11), with levels increasing until late gestation (Schmidt et al., 2000; Smas and Sul, 1993). At e12.5, *Dlk1* expression is high in the developing pituitary gland, pancreas, lung, adrenal gland, placenta, and many mesodermally-derived tissues, such as skeletal muscle and cartilage (da Rocha et al., 2007; Smas and Sul, 1993; Yevtodiyenko and Schmidt, 2006). In human embryos, *DLK1* expression mirrors that seen in the mouse, with adult expression restricted to specific cell types, including β-cells of the pancreas, somatotrophs of the pituitary gland, bone marrow, adrenal gland, and skeletal muscle (Floridon et al., 2000; Jensen et al., 1994; Jensen et al., 1993; Larsen et al., 1996; Schmidt et al., 2000; Tornehave et al., 1996).

1.2 Dlk1 functions to maintain undifferentiated cell populations

Studies performed in a variety of cell culture systems suggest that the primary role for DLK1 is to maintain the multipotency of progenitor cells until it is appropriate for them to differentiate. DLK1 function has been studied most extensively during the process of adipogenesis, the differentiation of preadipocyte cells to mature adipocytes. In preadipocyte cells, high levels of DLK1 coincide with ongoing proliferation and maintenance of the preadipocyte state. *Dlk1* is downregulated as adipogenesis begins, and forced expression of *Dlk1* at this time blocks preadipocyte differentiation (Smas and Sul, 1993). The specific functional roles of the membrane-bound and soluble forms of DLK1 remain unclear, however, and existing data is often contradictory (Boney et al., 1996; Garces et al., 1999; Mei et al., 2002; Nueda et al., 2007; Zhang et al., 2003). One extant hypothesis is that the membrane-bound and secreted forms of the protein play opposing roles in adipogenesis, and that the ratio of membrane-to-secreted protein determines whether cells proceed with differentiation (Garces et al., 1999).

1.3 Dlk1 associates with growth regulatory factors

The β-cells of the pancreas and the somatotrophs of the pituitary are neuroendocrine cells, producing circulating hormones under the control of signals from the nervous system. The β-cells produce Insulin in response to serum glucose levels, while the somatotrophs secrete Growth hormone (GH), the major endocrine regulator of postnatal growth. The interactions between DLK1, GH and Insulin are many and complex, with specific roles poorly defined. Abdallah et al reported an inverse correlation between serum DLK1 and GH, as mice with increased levels of circulating GH showed reduced amounts of the soluble DLK1 product FA1 (Abdallah et al., 2007). In rat preadipocytes, however, exogenous GH prevented the differentiation-induced downregulation of *Dlk1* expression and inhibited the differentiation process (Hansen et al., 1998). GH exerts many of its effects by stimulating production of Insulin-like growth factor I (IGF-I), and overexpression of DLK1 reduces IGF-I signaling, which reflects the ability of DLK1 to downregulate GH (Lupu et al., 2001; Zhang et al., 2003). Another layer of regulation may be present in the individual roles of the

transmembrane and soluble forms of DLK1, which have been little explored in these systems.

The placenta is also an endocrine tissue, and plays a major role in controlling fetal growth by the production of growth factors and through regulation of nutrient transfer to the fetus. Significant placental dysfunction invariably leads to fetal death, while milder defects result in growth retardation that can persist long after birth (Charalambous et al., 2007). We have shown previously that *Dlk1* is expressed in the fetal endothelial cells of the mid-gestation placental labyrinth, the site of maternal-fetal exchange (Yevtodiyenko and Schmidt, 2006). The function of *Dlk1* in the placental labyrinth is unknown, but is intriguing given the importance of the placenta in fetal growth and survival.

1.4 Mouse models define a role for Dlk1 in growth regulation

Several mouse models have been generated that display altered *Dlk1* expression, either in isolation or in combination with other linked imprinted genes, and these invariably show changes in growth. Previously described *Dlk1* null mice (*Dlk1*^{tm1Hsul}, referred to here as *Dlk1*$^{Sul\text{-}pat}$ to indicate paternal inheritance of the mutant allele) exhibit significant neonatal lethality, and animals surviving the neonatal period show growth retardation, skeletal defects and reduced adipose tissue as adults (Moon et al., 2002). *Dlk1*$^{Sul\text{-}pat}$ survivors are 14% smaller than wild type (WT) littermates at weaning, but attain a normal weight by 10 to 15 weeks of age (Moon et al., 2002). Two additional mouse models, *Gtl2lacZ* and *Gtl2Δ5′Neo,* have bacterially derived transgene sequences inserted in the *Maternally-expressed gene 3* (*Meg3*) imprinting control region located downstream of *Dlk1* (Schuster-Gossler et al., 1996; Sekita et al., 2006; Steshina et al., 2006). These models show partial early lethality and decreased growth, and reduced *Dlk1* levels have been demonstrated in both lines. Mice with a two-fold increase in *Dlk1* levels display developmental overgrowth and early postnatal lethality, while those expressing a three-fold *Dlk1* increase show embryonic lethality with edema and lung and skeletal defects (da Rocha et al., 2009).

When constitutive gene deletions produce complex phenotypes, identifying the tissues or cell types responsible for individual aspects of that phenotype can be difficult. This is particularly true when investigating systemic parameters such as survival and growth, which are regulated by processes originating within multiple systems. Conditional or “floxed” alleles allow the sequential examination of gene function in candidate cell types against a WT background. We generated a conditional allele for the *Dlk1* gene (*Dlk1*$^{tm1.1Jvs}$, referred to here as *Dlk1*^{flox}), to investigate the global aspects of the *Dlk1* null phenotype, focusing on the early lethality and growth effects. We identified three neuroendocrine sites of *Dlk1* expression as potentially causative for these phenotypes, the β-cells of the pancreas, the somatotrophs of the pituitary and endothelial cells, particularly the fetal endothelial cells of the placental labyrinth. As the process of producing mice with a conditional *Dlk1* allele also generates animals with a constitutive deletion (*Dlk1*$^{cons\text{-}pat}$), these mice were characterized and compared to the existing *Dlk1*$^{Sul\text{-}pat}$ animals, confirming and extending the *Dlk1* null phenotype.

2. RESULTS

2.1 Generation of Dlk1^{flox} and Dlk1^{cons} mice

A conditional *Dlk1* gene targeting vector was designed to flank exons 5 and 6 with loxP sites, to produce an allele that would allow both constitutive and conditional *Dlk1* deletions (Fig. 1). Exons 5 and 6 account for 77% of the DLK1 protein coding sequence, including four of six EGF-like domains and the transmembrane domain, and therefore this allele is expected to be a null. This is a significantly larger deletion than that present in the *Dlk1*$^{Sul\text{-}pat}$ mice, which have portions of exons 3 and 4 removed. The *Dlk1* targeting

construct was transfected into E14 embryonic stem (ES) cells and clones were selected using the neomycin analog G418. Surviving clones were screened by Southern blotting, and two correctly targeted clones were microinjected into C57BL/6 (B6) blastocysts. One clone yielded high percentage chimeras which were crossed to B6 females to achieve germline transmission. The resulting mice were designated *Dlk1*^{3lox}, and carried *Dlk1* exons 5 and 6 flanked by loxP sites, with a loxP-flanked Neo cassette (Fig. 1).

Dlk1^{3lox} mice were bred to EIIa-Cre animals, which express *Cre* recombinase from the one cell stage. The offspring from this cross carried one of three different recombination patterns upon genotyping, found in roughly equivalent proportions. Recombination between the loxP1 and loxP3 sites excised *Dlk1* exons 5 and 6 and the neomycin cassette, generating a *Dlk1* constitutive knockout mouse line (*Dlk1*^{cons}) (Fig. 1). Recombination between the loxP2 and loxP3 sites generated mice in which Neo was removed and exons 5–6 were flanked by loxP sites to allow subsequent conditional deletion (*Dlk1*^{flox}). Recombination between the loxP1 and loxP2 sites generated animals with an exon 5–6 deletion and Neo remaining in the locus; these mice were not experimentally useful and were not examined further.

Conditional alleles must retain normal activity after loxP insertion for them to be useful in tissue specific studies. To confirm that introducing loxP sites into the *Dlk1*^{flox} mice did not affect normal *Dlk1* expression, mRNA levels were examined by Northern blotting of embryos and placentae at e12.5 using a probe specific for *Dlk1* exon 6. Since *Dlk1* is expressed only from the paternally inherited allele, unless specified all analysis presented here was performed on paternal heterozygotes, animals in which the floxed allele was inherited paternally (*Dlk1*$^{flox\text{-}pat}$). Animals from the reciprocal cross, in which the floxed allele was inherited maternally (*Dlk1*$^{flox\text{-}mat}$), in addition to WT littermates from each cross, were used as controls. *Dlk1* levels in *Dlk1*$^{flox\text{-}pat}$ mice were not significantly different from WT, suggesting no effect of the loxP insertion (Fig. 2A, B). Northern analysis with the same exon 6 probe was also used to verify loss of *Dlk1* expression in animals inheriting the constitutive allele paternally (*Dlk1*$^{cons\text{-}pat}$), and *Dlk1* levels were found to be 7.3% and 3.7% of WT in embryos and placentae, respectively (Fig. 2C,D). This residual *Dlk1* signal represents basal expression from the imprinted maternal allele, a phenomenon observed at many imprinted loci (DeChiara et al., 1990; DeChiara et al., 1991; Schmidt et al., 1999; Zhang et al., 1993). This fact was confirmed by the complete loss of *Dlk1* mRNA in e12.5 homozygous *Dlk1*$^{cons\text{-}mat/pat}$ embryos and placentae (data not shown). The residual expression seen in *Dlk1*$^{cons\text{-}pat}$ mice does not rescue the *Dlk1* null phenotype, as *Dlk1*$^{cons\text{-}mat/pat}$ animals exhibit the same defects as those found in *Dlk1*$^{cons\text{-}pat}$ (data not shown).

2.2 Dlk1$^{cons\text{-}pat}$ mice display neonatal lethality and reduced growth

Survival and growth were examined in *Dlk1*$^{cons\text{-}pat}$ and *Dlk1*$^{cons\text{-}mat}$ mice at weaning (3 weeks of age). Crosses between B6 females and *Dlk1*^{cons} males gave a total of 86/137 (63%) WT and 51/137 (37%) *Dlk1*$^{cons\text{-}pat}$ offspring at weaning. The expected percentage of *Dlk1*$^{cons\text{-}pat}$ offspring from this cross is 50%, indicating a loss of 26% of the paternal knockout animals. All litters were counted at birth, and pups were often lost from this cross in the first few days, but were typically cannibalized before they could be recovered. It is likely many of these pups represent the missing *Dlk1*$^{cons\text{-}pat}$ animals. The *Dlk1*$^{cons\text{-}pat}$ mice therefore show reduced neonatal lethality in comparison to the *Dlk1*$^{Sul\text{-}pat}$ mice, where 50% of pups are reported to have died before weaning. In the *Dlk1*^{Sul} line, most lethality was reported to have occurred within the first two days after birth, but data was not given for this parameter so direct comparisons cannot be made (Moon et al., 2002). Crosses between *Dlk1*^{cons} females and B6 males yielded 55/112 (49%) WT and 57/112 (51%) *Dlk1*$^{cons\text{-}mat}$

offspring at weaning. Maternal inheritance of the *Dlk1*^{cons} allele therefore carries no increased risk of neonatal death.

Dlk1$^{cons\text{-}pat}$ mice that survived the neonatal period weighed significantly less than their WT littermates from one to six weeks of age (Fig. 3A). Female and male mice were analyzed separately for growth throughout these studies, as sex-specific differences begin to emerge before weaning. At postnatal day 7 (P7), *Dlk1*$^{cons\text{-}pat}$ female and male pups weighed 81% and 84% of WT, respectively, and this proportion increased to 89% and 87% by P42 (Fig. 3A). Surviving *Dlk1*$^{Sul\text{-}pat}$ animals also displayed growth retardation, weighing 85% of WT at weaning (Moon et al., 2002). To examine whether the *Dlk1* null growth phenotype begins during embryonic development, *Dlk1*$^{cons\text{-}pat}$ embryos were weighed at e12.5, e14.5 and e16.5, but showed no significant differences from WT (Fig. 3B). The *Dlk1*$^{cons\text{-}pat}$ dwarfism therefore begins during late gestation or shortly after birth. *Dlk1*$^{cons\text{-}mat}$ male mice weighed significantly less than WT littermates at P14, but this difference was not observed at other time points, or in *Dlk1*$^{cons\text{-}mat}$ female mice, and was not investigated further (Fig. 3A). Overall, maternal inheritance of the *Dlk1*^{cons} allele results in no change in growth.

2.3 Placental morphology is altered in Dlk1$^{cons\text{-}pat}$ mice

Detailed histological analysis was performed on all major tissues from six-week-old *Dlk1*$^{cons\text{-}pat}$ and *Dlk1*$^{cons\text{-}mat}$ mice, and their WT littermates. Brain, pituitary, adrenal gland, skeletal muscle (tongue), thymus, heart, lung, liver, spleen, kidney, pancreas, small intestine, retroperitoneal/inguinal fat pads, reproductive fat pads, and testis were examined (n = 3 for each *Dlk1*^{cons} and WT). With the exception of placentae and fat pads (discussed below and in section 2.4, respectively), no significant histological differences were detected in any tissues (data not shown).

Dlk1 is strongly expressed in the fetal vasculature of the labyrinthine layer of the mouse placenta (Yevtodiyenko and Schmidt, 2006). Placental defects in mice can cause fetal death or reduced size at birth, similar to that seen in *Dlk1* null mice, and defects in the analogous villous layer of the human placenta lead to developmental defects and fetal death (Anson-Cartwright et al., 2000; Kingdom et al., 2000). Placental weight was analyzed in *Dlk1*$^{cons\text{-}pat}$ animals at e12.5, e14.5, and e16.5, but no significant differences were observed from WT (Fig. 3B). Placental morphology was examined by histology of e12.5 *Dlk1*$^{cons\text{-}pat}$ placentae in comparison to their WT littermates (Fig. 4A–D). *Dlk1*$^{cons\text{-}pat}$ placentae had a labyrinth layer that was reduced in size, comprising an average of 62% of the total placental area, compared to 72% for WT animals (p=0.04)(Fig. 4A–D and data not shown). As overall placental size was unchanged, the junctional (spongiotrophoblast) zone of *Dlk1*$^{cons\text{-}pat}$ placentae was correspondingly increased, to 38% of total placental size compared to 28% in WT animals (p=0.04)(Fig. 4A–D and data not shown). Histologically, the *Dlk1*$^{cons\text{-}pat}$ placental labyrinth showed increased cellularity and decreased vascularity in comparison to WT, and the junctional zone had a decreased number of glycogen cells with an increase in pre-glycogen cells. *In situ* hybridization using a probe for the spongiotrophoblast-specific marker *Tpbpa*, the Trophoblast-specific protein alpha, allowed visualization of the altered labyrinth-spongiotrophoblast ratio in *Dlk1*$^{cons\text{-}pat}$ placentae (Fig. 4E, F).

2.4 Dlk1 deficient mice demonstrate altered adipose tissue

Dlk1$^{Sul\text{-}pat}$ mice had normal fat pad weights at 8 weeks of age, but at 16 weeks on a high fat diet, these mice showed a significant increase in fat pad weight (Moon et al., 2002). Fat pad development was scored in *Dlk1*^{cons} mice by weighing the retroperitoneal/inguinal and reproductive fat pads from six week old mice fed a normal diet. Several changes from WT were observed in female *Dlk1*^{cons} animals, but these changes were never seen in males and did not correlate with loss of *Dlk1*. A significant decrease was observed in retroperitoneal/

inguinal fat pad weight, as a percentage of total body weight, in both female *Dlk1*$^{cons\text{-}pat}$ and female *Dlk1*$^{cons\text{-}mat}$ mice compared to WT littermates (Fig. 5A). *Dlk1*$^{cons\text{-}mat}$ mice also showed a decrease in parametrial fat pad weight (Fig. 5A). Changes in *Dlk1*$^{cons\text{-}mat}$ mice cannot be a result of loss of *Dlk1*, however, as these animals have normal *Dlk1* levels. Despite this lack of *Dlk1*-dependent fat pad weight changes in *Dlk1*^{cons} mice, histological analysis showed that both male and female *Dlk1*$^{cons\text{-}pat}$ mice had hypotrophic adipocytes in all fat pads at 6 weeks of age (Fig. 5B). Adipocyte size varies widely between individual fat pads, and across different regions of a single fat pad, so average adipocyte size was quantified by measuring cell volume in histological sections using ImageJ software. *Dlk1*$^{cons\text{-}pat}$ adipocytes averaged only 686 μm^2 in size, while WT animals had an average adipocyte size of 849 μm^2 ($p<0.001$) (Fig. 5C). At 16 weeks the phenotype had resolved, and WT and *Dlk1*$^{cons\text{-}pat}$ adipocytes were equal in size (1340 μm^2 and 1328 μm^2, respectively) (Fig. 5C).

2.5 Dlk1 deletion in pancreatic β-cells does not affect neonatal survival or growth

Mice lacking any one of several genes in the Insulin pathway show reduced birth weight, with perinatal lethality from ketoacidosis occurring approximately 48 hours after birth (Accili et al., 1996; Duvillie et al., 1997; Joshi et al., 1996). The timing of this lethality is similar to that seen in *Dlk1*$^{Sul\text{-}pat}$ and *Dlk1*$^{cons\text{-}pat}$ animals, and suggested that alterations in Insulin signaling during the critical newborn period might underlie the *Dlk1* null lethality. *Dlk1* is highly expressed in the β-cells of the pancreatic islets, and has multiple roles in regulating the Insulin/IGF-1 signaling pathway (Garces et al., 1999; Nueda et al., 2008).

To assay the role of *Dlk1* in pancreatic β-cells, a β-cell-specific *Dlk1* deletion (called *Dlk1*^{Ins}) was generated by crossing *Dlk1*^{flox} mice to the transgenic line *rIP-Cre*, which expresses Cre recombinase from the rat Insulin II promoter (Postic et al., 1999). *rIP-Cre* mice have been reported to show some degree of glucose intolerance on their own, and the use of *rIP-Cre* controls is recommended to minimize any impact of this potentially confounding factor (Lee et al., 2006). To control for any effect that the *Cre* transgene itself may have on mouse development, *Dlk1*^{Ins} mice were therefore compared to littermates that were WT for *Dlk1* but heterozygous for the *rIP-Cre* transgene (Lee et al., 2006).

Dlk1$^{Ins\text{-}pat}$ mice, who carry a paternally-inherited *Dlk1* deletion specifically in pancreatic β-cells, are fully viable; crosses between *rIP-Cre* females and *Dlk1*^{flox} males yielded 39/91 (43%) *rIP-Cre* control offspring and 52/91 (57%) *Dlk1*$^{Ins\text{-}pat}$ offspring at weaning. The apparent higher survival of *Dlk1*$^{Ins\text{-}pat}$ offspring is likely an artifact of the relatively small numbers of animals analyzed. *Dlk1*$^{Ins\text{-}pat}$ mice also showed no change in growth from one to six weeks of age, though male *Dlk1*$^{Ins\text{-}pat}$ mice did appear significantly heavier than control mice at one time point, P7 (Fig. 6A). This difference is not observed in females or in either sex at other time points, and was not explored further. The reciprocal cross generated 80/147 (54%) *rIP-Cre* animals and 67/147 (46%) *Dlk1*$^{Ins\text{-}mat}$ animals; there was no difference in weight between these two groups, indicating no effect of a maternal *Dlk1* β-cell deletion (Fig. 6A). Under histological analysis, *Dlk1*$^{Ins\text{-}pat}$ mice showed no changes in the size, number or morphology of adult islets, and all other tissues examined were normal (Fig. 6B, C and data not shown).

To confirm that Cre-mediated excision in *rIP-Cre* mice was specific to the β-cells of the pancreas, and to verify the extent of Cre excision directed by this transgene, *rIP-Cre* mice were crossed to the B6.129S4-*Gt(ROSA)26Sor*^{tm1Sor}/J reporter mouse line (referred to as *ROSA26*). In these mice, Cre recombinase excises a floxed stop codon to allow *lacZ* expression in cells where *Cre* is active (Soriano, 1999). Pancreases from offspring of the *rIP-Cre/ROSA26* cross were collected and analyzed for β-galactosidase activity at 6 weeks of age. In previous reports, *rIP-Cre* mice have been reported to excise a floxed gene in 82%

of β-cells. Counting β-galactosidase positive cells in histological sections of *rIP-Cre/ROSA26* pancreases showed 72% (413/572) of islet cells expressed *lacZ*, a number consistent with the estimate that 70–85% of islets are β-cells (Fig. 6D, E) (Gannon et al., 2000).

Immunohistochemistry with an antibody against DLK1 was then used to verify the loss of DLK1 from islet cells in $Dlk1^{Ins\text{-}pat}$ pancreases compared to *rIP-Cre/+* controls (Fig. 6F-I). DLK1 levels in control islet cells were low but detectable, as expected in adult animals. Interestingly, high levels of DLK1 were seen in the acinar cells surrounding the islets, a tissue not previously shown to express DLK1 (Fig. 6F, H). $Dlk1^{Ins\text{-}pat}$ mice show a virtually complete loss of DLK1 in the islets, confirming the efficiency of the rIP-Cre-mediated excision, and a significant decrease in acinar cell DLK1 (Fig. 6G, I). Loss of much of the DLK1 signal in the acinar cells indicates that the DLK1 present in WT pancreatic acini may originate from the β-cells, produced as a soluble protein form that is secreted to adjacent cells.

2.6 Dlk1 deletion in pituitary somatotrophs does not affect neonatal survival or growth

Mice deficient in the growth hormone (*Gh*), growth hormone receptor (*Ghr*), or growth hormone receptor/binding protein genes (*Ghr/bp*) display a proportional dwarfism similar to that observed in *Dlk1* null mice (Amselem et al., 1989; Wajnrajch et al., 1996; Zhou et al., 1997). *Dlk1* is expressed in the developing pituitary gland at e12.5, becoming restricted to the GH-producing somatotrophs of the mature pituitary (Larsen et al., 1996; Yevtodiyenko and Schmidt, 2006). DLK1 is involved in GH regulation, but data on the specific relationship between DLK1 and GH are often contradictory, likely due to observations being made in different tissues or at differing points in development (Abdallah et al., 2007; Ansell et al., 2007; Carlsson et al., 1997; Hansen et al., 1998; Wolfrum et al., 2003). Given these data, we hypothesized that the growth retardation of $Dlk1^{cons\text{-}pat}$ and $Dlk1^{Sul\text{-}pat}$ mice could be due to reduced GH signaling.

To assay the role of DLK1 in GH-producing somatotrophs, a somatotroph-specific *Dlk1* deletion (called $Dlk1^{Gh}$) was generated by crossing $Dlk1^{flox}$ mice to the transgenic line *rGh-Cre*, which expresses *Cre* recombinase from the rat Growth hormone promoter (Luque et al., 2007). To control for any effect of the *Cre* transgene, $Dlk1^{Gh}$ mice were compared to littermates that were WT for *Dlk1* but heterozygous for the *rGh-Cre* transgene (Lee et al., 2006).

$Dlk1^{Gh\text{-}pat}$ mice, who carry a paternally-inherited *Dlk1* deletion specifically in pituitary somatotrophs, are fully viable; crosses between *rGh-Cre* females and $Dlk1^{flox}$ males yielded 39/88 (44%) *rGh-Cre* control offspring and 49/88 (56%) $Dlk1^{Gh\text{-}pat}$ offspring at weaning. $Dlk1^{Gh\text{-}pat}$ mice showed no reproducible change in growth from one to six weeks of age, though at six weeks female $Dlk1^{Gh\text{-}pat}$ mice were found to be significantly smaller than *rGh-Cre* control females (Fig. 7A). This difference was not observed in males, or in either sex at other time points, and was not considered further. The reciprocal cross generated 40/78 (51%) *rGh-Cre* control offspring and 38/78 (49%) $Dlk1^{Gh\text{-}mat}$ offspring at weaning, and there was no difference in weight between these two groups, indicating no effect of a maternal *Dlk1* somatotroph deletion (Fig. 7A and data not shown). Under histological analysis, $Dlk1^{Gh\text{-}pat}$ mice showed no changes in the size or morphology of the adult pituitary, and with one exception all other tissues examined were normal (Fig. 7B, C and data not shown). In 6 week old male $Dlk1^{Gh\text{-}pat}$ mice, retroperitoneal/inguinal fat pads weighed significantly more than *rGh-Cre* control fat pads (data not shown). This difference was not observed in female $Dlk1^{Gh\text{-}pat}$ mice, and is likely an artifact of the relatively small sample size.

To confirm that Cre-mediated excision in *rGh-Cre* mice was specific to pituitary somatotrophs, and to verify the extent of Cre excision directed by this transgene, *rGh-Cre* mice were crossed to the *ROSA26* reporter line. Pituitaries from offspring of the *rGh-Cre*/*ROSA26* cross were collected and analyzed for β-galactosidase activity at 6 weeks of age. β-galactosidase activity was seen in the anterior lobe of the pituitary, but absent from the posterior pituitary in these mice (Fig. 7D, E). The weak β-galactosidase activity seen at the edges of the intermediate lobe is believed to be bleedover resulting from the very strong anterior pituitary expression. *rGh-Cre* mice have been reported to excise a floxed gene in ~99% of GH-producing cells of the anterior pituitary gland, but not in other anterior pituitary cell types such as gonadotropes or corticotropes (Luque et al., 2007). Counting β-galactosidase positive cells in histological sections of pituitaries showed 45.2% (358/792) of anterior pituitary cells expressing *lacZ*, consistent with the estimate that somatotrophs comprise 40–50% of the anterior cells (Gannon et al., 2000). Immunohistochemistry with the DLK1 antibody was used to confirm DLK1 presence in *rGh-Cre/+* control pituitaries (Fig, 7F, H), and its loss in $Dlk1^{Gh\text{-}pat}$ pituitaries (Fig. 7G, I). Additionally, fluorescence activated cell sorting was used to isolate somatotrophs from $Dlk1^{Gh\text{-}pat}$ and control littermate pituitaries using a GH antibody. DNA was extracted from both cell populations and a region spanning the exon 5/6 deletion was amplified by PCR using primers within loxP1 and downstream of *Dlk1* exon 6 (Fig. 1). Sequencing of the product amplified from $Dlk1^{Gh\text{-}pat}$ cells confirmed the excision of *Dlk1* exons 5 and 6 in this target tissue (data not shown).

To determine if loss of *Dlk1* expression in somatotrophs alters *Gh* levels, quantitative reverse transcription polymerase chain reaction (qRT-PCR) was used to analyze levels of *Dlk1* and *Gh* mRNA in total adult mouse pituitary. In $Dlk1^{Gh\text{-}pat}$ mice, *Dlk1* expression was decreased to 28% of control levels (Fig. 7J). The residual *Dlk1* expression is likely due to low levels of *Dlk1* expression from the intermediate and posterior lobes of the pituitary, and/or incomplete excision in a small population of somatotrophs (Larsen et al., 1996; Yevtodiyenko and Schmidt, 2006). Growth hormone mRNA levels were unchanged in $Dlk1^{Gh\text{-}pat}$ mice, which correlates with the lack of a growth defect in these animals, and indicates that *Dlk1* is not required for *Gh* expression in somatotrophs (Fig. 7J).

2.7 Dlk1 deletion in endothelial cells does not affect neonatal survival or growth

Dlk1 is expressed in endothelial cells in a variety of embryonic tissues and in the fetal-derived endothelium of the placental labyrinth (Bondjers et al., 2006; Jensen et al., 1994; Yevtodiyenko and Schmidt, 2006). In adipose and skeletal muscle, two tissues that express high levels of *Dlk1*, the expressing cells have been shown to include the endothelial cells of the stroma (Andersen et al., 2009a; Andersen et al., 2009b; Waddell et al., 2010). These data suggested a previously unexpected role for *Dlk1* production in the vasculature of expressing tissues, where it might exert key functions by acting in a paracrine manner on adjacent cell types. Particularly in the placenta, *Dlk1* expression in the labyrinth endothelium could indicate a key role in regulating embryonic growth.

To assay the role of *Dlk1* in endothelial cells, endothelial-specific *Dlk1* deletions ($Dlk1^{Tie1}$ and $Dlk1^{Tie2}$) were generated by crossing $Dlk1^{flox}$ mice to the transgenic lines *Tie1 (Tunica intima endothelial kinase 1)-Cre* and *Tie2-Cre*, which express Cre recombinase under the control of the mouse *Tie1* and *Tie2* promoters, respectively (Gustafsson et al., 2001; Koni et al., 2001). We were interested specifically in the role of *Dlk1* in placental endothelial cells, yet a promoter unique to this population of cells has not yet been described. The *Tie1* and *Tie2* genes are both expressed in placental endothelium, and in overlapping patterns of fetal endothelial cells, with *Tie2* having a more widespread distribution (Gustafsson et al., 2001; Koni et al., 2001). *Tie1-Cre* mediated excision has exhibited 70–90% efficiency in adult kidney, liver and brain and 90–95% efficiency in lung and heart (Gustafsson et al., 2001).

Tie2-Cre has demonstrated 85–100% excision in bone marrow cells, 100% in lymph node vasculature, 84% of early hematopoietic progenitors, and 82% of blood cells in the embryonic yolk sac (Koni et al., 2001; Tang et al., 2010). Conditional deletions were generated using both Cre transgenic lines due to concern that a broad *Dlk1* deletion in fetal endothelium might obscure any placental effect, while a consistent phenotype from both deletions would suggest a placental cause. To control for any effect of the *Cre* transgenes, $Dlk1^{Tie1}$ and $Dlk1^{Tie2}$ mice were compared to control littermates that were WT for *Dlk1* but heterozygous for the *Tie1-Cre* or *Tie2-Cre* transgenes (Lee et al., 2006).

$Dlk1^{Tie1\text{-}pat}$ and $Dlk1^{Tie2\text{-}pat}$ mice, who carry paternally-inherited deletions of the *Dlk1* gene specifically in endothelial cells, are fully viable; crosses between *Tie1* or *Tie2* females and $Dlk1^{flox}$ males respectively yielded 36/83 (43%) control offspring and 47/83 (57%) $Dlk1^{Tie1\text{-}pat}$ offspring, and 51/102 (50%) control offspring and 51/102 (50%) $Dlk1^{Tie2\text{-}pat}$ offspring at weaning. The reciprocal cross produced 45/79 (57%) control offspring and 34/79 (43%) $Dlk1^{Tie1\text{-}mat}$ and 35/55 (64%) control offspring and 20/55 (36%) $Dlk1^{Tie2\text{-}mat}$ offspring at weaning. $Dlk1^{Tie\text{-}mat}$ mice do not have altered levels of *Dlk1*, so the apparent loss of $Dlk1^{Tie\text{-}mat}$ mice in both crosses is likely a result of relatively small numbers of mice analyzed. $Dlk1^{Tie1}$ and $Dlk1^{Tie2}$ mice showed no differences in body weight in comparison to control animals up to 6 weeks of age, indicating no effect of a *Dlk1* deletion in endothelial cells (Fig. 8A, B). The loss of DLK1 from placental endothelial cells was confirmed by immunohistochemistry using a DLK1 antibody on $Dlk1^{Tie1\text{-}pat}$ placentae in comparison to control placentae (Fig. 8C–F). This analysis showed significant reduction in DLK1 levels in $Dlk1^{Tie1\text{-}pat}$ placenta, indicating efficient *Tie1-Cre*-mediated *Dlk1* excision. As no survival or growth phenotype was seen in these animals the placental structure was not analyzed histologically.

3. DISCUSSION

Mice lacking *Dlk1* display a complex developmental phenotype, most intriguingly a partially penetrant neonatal lethality with proportional dwarfism of the survivors. Changes in systemic parameters such as survival and growth reflect the expression profile of *Dlk1* in neuroendocrine tissues, which produce paracrine or endocrine circulating hormones. Systemic phenotypes are among the most difficult to study, however, and the identification of the specific causative tissue or cell type can require the production of complex animal models. The ability to generate tissue-specific deletions using floxed alleles in gene targeted mice has greatly simplified this process. In this work, we have used four separate conditional mouse deletions to explore the requirement for *Dlk1* in three discrete cell types. We show, surprisingly, that none of these cell types, primary candidates for *Dlk1* systemic functional roles, are responsible for the lethality or the growth defects of $Dlk1^{cons\text{-}pat}$ mice. The cell type(s) that employ *Dlk1* in the regulation of these key developmental parameters remain to be identified.

3.1 Dlk1 null mice display neonatal lethality and growth retardation

$Dlk1^{cons\text{-}pat}$ mice carrying an exon 5–6 deletion largely recapitulate the lethality and dwarfism seen in the previously described $Dlk1^{Sul\text{-}pat}$ mice, but show differences in the appearance of placental and adipose tissue. Significantly, we analyzed the placentae of $Dlk1^{cons}$ mice, a tissue that was not studied in $Dlk1^{Sul\text{-}pat}$ animals. Histological analysis of $Dlk1^{cons\text{-}pat}$ placentae revealed subtle but consistent morphological changes in the placental labyrinth, including a smaller labyrinth with a reduced vascular compartment that may act to alter maternal nutrient provisioning to the developing fetus. Placental function is key to proper embryonic and postnatal development, and further examination of placental *Dlk1* function is warranted.

Dlk1$^{cons\text{-}pat}$ mice had fat pads of normal weight, but showed a decrease in individual fat cell size when fed a standard diet. Despite having hypotrophic fat cells, *Dlk1*$^{cons\text{-}pat}$ mice were still able to correct their early growth deficit to some extent, attaining 88% of WT weight at 6 weeks of age. *Dlk1*$^{Sul\text{-}pat}$ mice displayed increased fat pad weight, hypertrophic adipocytes, and increased lipid metabolite levels in 16 week old animals fed a high fat diet (Moon et al., 2002). Paradoxically, transgenic mice overexpressing *Dlk1* and fed a high fat diet exhibit hypotrophic adipocytes similar to what is observed in *Dlk1*$^{cons\text{-}pat}$ animals (Villena et al., 2008). Differences in age and diet likely explain these differences, and support complex and changing roles for *Dlk1* in adipogenesis.

3.2 Dlk1 is dispensable in multiple expressing tissues

Analysis of the *Dlk1*^{Ins}, *Dlk1*^{Gh}, *Dlk1*^{Tie1}, and *Dlk1*^{Tie2} conditional knockout mice led us to conclude that the neonatal lethality and weight deficiency observed in the *Dlk1*^{cons} mice does not result from the loss of *Dlk1* expression in β-cells of the pancreas, somatotrophs of the pituitary, or endothelial cells. The cell types targeted were those in which *Dlk1* is known or believed to be involved in pathways that could underlie neonatal death and/or growth retardation. Our hypothesis was that the loss of *Dlk1* in β-cells would result in neonatal lethality, while loss in somatotrophs would result in growth deficiency. Absence of *Dlk1* from endothelial cells, particularly those in the placental labyrinth, could contribute to both lethality and growth defects. As none of the cell-specific deletions recapitulated these parameters as seen in *Dlk1*$^{cons\text{-}pat}$ mice, and uncovered no additional phenotypes, we conclude that *Dlk1* expression in these cell types is not required for normal growth and survival.

3.3 Roles for Dlk1 in development and growth

The surprising findings that the most obvious parameters of the *Dlk1* null phenotype cannot be recapitulated by individual deletions in several predominant *Dlk1*-expressing tissues calls for a reevaluation of the biological roles attributed to *Dlk1*. There are several possible explanations for the origin of the *Dlk1*$^{cons\text{-}pat}$ phenotype, and the inability of these conditional deletions to reproduce its effects. First, it is possible that much of the *Dlk1*$^{cons\text{-}pat}$ phenotype derives solely or largely from expression in a key tissue not yet examined. One candidate is the adrenal gland, as *Dlk1* is expressed both in the chromaffin cells of the adrenal medulla, and in the cortical zona glomerulosa (Yevtodiyenko and Schmidt, 2006). The adrenal gland functions to regulate physiological parameters such as electrolyte balance and stress responses. *Acd* (*Adrenocortical dysplasia*) mice display abnormal adrenal cortex morphology with reduced levels of glucocorticoids; these mice are 55–65% of normal weight at birth and 40% of mutants die within 24 hours (Heikkila et al., 2002). *Wnt4* (*Wingless-type MMTV integration site family, member 4*) mutant mice show significantly reduced aldosterone levels without obvious histological change in the zona glomerulosa (Beamer et al., 1994). *Wnt4* mice die soon after birth, but the multiple defects they present makes it difficult to ascribe the cause to adrenal dysfunction. *Dlk1* null mice show no overt adrenal changes by histology, but as the *Wnt4* mice demonstrate, dysplasia is not strictly required for adrenal dysfunction.

Recent work has shown that *Dlk1* is expressed at high levels in undifferentiated brown adipose tissue (BAT), with expression peaking during late embryogenesis and then declining (Armengol et al., 2012; Hernandez et al., 2007). *Dlk1*$^{Sul\text{-}pat}$ mice display increased expression of thermogenesis genes in the neonatal period, and decreased lipid accumulation in brown adipose cells (Armengol et al., 2012). In *Gtl2lacZ*^{mat} mice, increased *Dlk1* expression results in failure of BAT to properly differentiate, and reduced expression of thermogenesis genes (Charalambous et al., 2012). These data point to *Dlk1* as a key regulator of BAT differentiation that controls the capacity for thermogenesis as a

mechanism of temperature regulation. Thermogenesis is critical for temperature regulation during the early postnatal period, suggesting that alterations in this process could be involved in the varied developmental phenotypes of both *Dlk1* null mice. A BAT-specific *Dlk1* deletion could be very informative.

Second, it is possible that *Dlk1* is required in one or more of the tissues examined, but that loss of expression in the specific cell type targeted is masked by paracrine expression from other cell types in the same tissue. Deletion of *Dlk1* specifically in myoblasts of developing skeletal muscle (*Dlk1*^{Skm}), for example, showed that *Dlk1* expression in whole muscle was decreased to only 65% of control, with the remaining expression derived primarily from endothelial cells within the muscle (Waddell et al., 2010). Stromal cells in other tissues may similarly compensate for *Dlk1* loss in known signaling cells. In the pituitary for example, *Dlk1* is expressed in some cells of the intermediate lobe, which might compensate for loss in the anterior somatotrophs. Similarly, *Dlk1* expression has been detected in the stroma and acini of e15–16 mouse pancreas, which might compensate for *Dlk1* loss in β-cells (da Rocha et al., 2007).

Third, it is possible that *Dlk1* is required in one or more of the cell types analyzed, but that loss of *Dlk1* expression is compensated by the related gene *Dlk2* (Nueda et al., 2007). Only recently identified, the function of *Dlk2* is not well understood, but its expression pattern shows some overlap with that of *Dlk1*. Both genes are expressed during embryonic development, although *Dlk2* expression is activated primarily during late gestation, while *Dlk1* is expressed from at least e11. *Dlk2* has been shown to be expressed in the placenta, but expression in the pituitary and pancreas have not been analyzed (Nueda et al., 2007). While preliminary experiments have suggested that DLK2 functions to oppose DLK1 during adipogenesis, its activities in other cell types are unknown.

Lastly, it is possible that systemic parameters such as survival and growth are under the control of *Dlk1* produced by more than one of the tissues analyzed, and that the effects of loss of *Dlk1* in any one tissue is compensated in an endocrine manner by *Dlk1* production from another tissue. Recapitulating the *Dlk1*$^{cons\text{-}pat}$ phenotype would then require combinatorial deletion in multiple individual tissue types.

4. EXPERIMENTAL PROCEDURES

4.1 Targeting construct design

The ploxPneo-1 plasmid (Nagy et al., 1998) contains two loxP sites flanking a *Phosphoglycerate kinase 1* (*Pgk1*) promoter driven neomycin cassette. A third loxP site was ligated into the *Sal*I restriction site upstream of the *Pgk-1* promoter generating the plasmid p3loxNeo. The 28G5 BAC clone (CHORI, Oakland, CA), spanning 3.5 kb upstream of *Dlk1* to 69 kb downstream of the *Meg3*, was used to isolate the mouse *Dlk1* gene and its surrounding genomic sequence (Schmidt et al., 2000). Three DNA fragments, a 3.3 kb *Not*I/*Eco*RI fragment, a 4.6 kb *Eco*RI/*Bam*HI fragment, and a 2.4 kb *Bam*HI/*Bam*HI fragment, were excised from 28G5 and ligated into the unique *Bam*HI, *Nhe*I, and *Kpn*I sites of p3loxNeo, respectively. The resulting p3loxΔDlk1 targeting construct contains three regions of homology to *Dlk1* as well as a neomycin cassette.

4.2 Generation of Dlk1^{3lox} mice

The targeting construct was linearized using *Not*I, transfected into E14 embryonic stem cells, and selected using G418. Neomycin resistant clones were screened for homologous recombination using Southern blot analysis, as previously described (Yevtodiyenko et al., 2004). ES cell DNA was digested with *Hind*III or *Bst*EII and probed with a 1.3 kb *Dra*I/*Xcm*I probe corresponding to a region in the 5′ flanking region of *Dlk1*. This assay detected

a 9 kb WT or 7 kb targeted band. Targeting of the 3′ flank was confirmed using a 1 kb *Bam*HI/*Xcm*I probe that would bind to a 5 kb WT or 7 kb targeted band. Cells possessing the targeted allele were then microinjected into C57BL/6 (B6) mouse blastocysts to generate chimeric offspring, which were backcrossed to B6 mice to transmit the mutation ($Dlk1^{3lox}$) through the germ line. $Dlk1^{3lox}$ mice were genotyped by PCR of tail DNA using the following primers located in *Dlk1* intron 4 and loxP1, respectively: OL657 – 5′ AGCAGCAGCTACTTGTTTGGG 3′; OL706 – 5′ TGGCTGGACGTAAACTCCTCTT 3′.

4.3 Mice and genotyping

EIIa-Cre mice, which express *Cre* recombinase under the control of the adenovirus *EIIa* promoter (*B6.FVB-Tg(EIIa-Cre)C5379Lmgd/J*, strain #003724) (Lakso et al., 1996), were purchased from the Jackson Laboratory (Bar Harbor, Maine, USA) and were bred to the $Dlk1^{3lox}$ mice to excise the neomycin cassette and generate the *Dlk1* floxed ($Dlk1^{tm1.1Jvs}$, here denoted as $Dlk1^{flox}$) and constitutive knockout ($Dlk1^{cons}$) mice. These mice were genotyped by PCR using the following primers located immediately downstream of *Dlk1* exon 6 and in loxP3, respectively: $Dlk1^{flox}$, OL1512 – 5′ GCTGCAGGTCGTCGTCGAAATTCC 3′; OL655 – 5′ TTCCCAAACTGGACATGAGCCA 3′; $Dlk1^{cons}$, OL657 and OL655. PCR was performed on an Eppendorf Mastercycler (Hamburg, Germany) as follows: 95°C for 5 minutes, 35 cycles of 94°C for 30 seconds, 63°C for 30 seconds, 72°C for 30 seconds, and 72°C for 10 minutes. The $Dlk1^{flox}$ product is 200 bp, while the $Dlk1^{cons}$ product is 400 bp. The rat Insulin promoter Cre recombinase (*rIP-Cre*) mice (*B6.Cg-Tg(Ins2-Cre)25Mgn/J*, strain #003573) were purchased from Jackson Laboratory (Bar Harbor, Maine, USA). The rat *Gh* promoter-Cre recombinase (*rGh-Cre*) mice were provided by Rhonda Kineman of the University of Illinois at Chicago (Luque et al., 2007) and were maintained on a B6 background. The *Tie1-Cre* mice were provided by Kai Jiao at the University of Alabama. The *Tie2-Cre* mice (*B6.Cg-Tg(Tek-Cre)12Flv/J*, stock #004128) were purchased from Jackson Laboratory (Bar Harbor, Maine, USA). All Cre mice were genotyped using the primers: OL1227 – 5′ CGTACTGACGGTGGGAGAAT 3′; OL1228 – 5′ CCCGGCAAAACAGGTAGTTA 3′ which amplify a 166 bp product. The *B6.129S4-Gt(ROSA)26Sor*^{tm1Sor}*/J* mice (strain #003474) mice were purchased from Jackson Laboratory (Bar Harbor, Maine, USA) on a B6 background. Mice were genotyped using the primers: OL1041 – 5′ GCGAAGAGTTTGTCCTCAACC 3′; OL1042 – 5′ GGAGCGGGAGAAATGGATATG 3′; OL1043 – 5′ AAAGTCGCTCTGAGTTGTTAT 3′ which produces a 650 bp WT product while the mutant allele produces a 340 bp product.

4.4 Northern analysis

Embryos and placentae were dissected and their genotypes were determined by PCR of yolk sac DNA. Total RNA was extracted using TRIzol reagent (Invitrogen, Carlsbad, CA, USA), purified by phenol:chloroform:isoamyl alcohol extraction and ethanol precipitation, and Northern blotting was performed, as previously described (Steshina et al., 2006). Blots were imaged with a Storm Phosphorimager and results were quantified using ImageQuant 5.2 analysis software (GE Healthcare, Piscataway, NJ, USA). The probes for *Dlk1* and *β-actin* were amplified by RT-PCR using the primers: *Dlk1*, OL56 – 5′ ATGGCGTCTGCACCGACATC 3′; OL57 – 5′ CACACAATAGAGCAAACTCCACCAC 3′; *β-actin*, OL1514 – 5′ TGTGATGGTGGGAATGGGTCAGAA 3′; OL1515 – 5′ TGATGTCACGCACGATTTCCCTCT 3′. The *Dlk1* probe is specific to a region on exon 6 and the *β-actin* probe binds to a region spanning exons 3–5. RT-PCR products were run on a 0.8% agarose gel and isolated using QIAquick column purification (Qiagen, Valencia, CA, USA). Probes were radiolabeled by incubation of 50 ng of DNA with 2 u Klenow enzyme, 50 μCi α-^{32}P, 20 μg BSA, and 10 μL of oligo labeling buffer for 1 hour to overnight at room temperature (RT). The radiolabeled probe was purified on a Sephadex G50 spin

column (Roche, Indianapolis, IN, USA) and the intensity of radioactivity was determined using a LG6500 Multi-Purpose scintillation counter (Beckman Coulter, Brea, CA, USA).

4.5 Measurement of animal and tissue weight

Mice were fed a normal diet after weaning consisting of ≥ 5% crude fat (Harlan Teklad LM-485 Mouse/Rat Diet 7912). The mice were weighed at weekly intervals from one to six weeks after birth. In the *rIP-Cre*, *rGh-Cre*, *Tie1-Cre*, and *Tie2-Cre* crosses, pups carrying one copy of the $Dlk1^{flox}$ allele and heterozygous for Cre recombinase (+/$Dlk1^{flox}$; *Cre*/+) were compared to mice heterozygous for *Cre* recombinase alone (+/+; *Cre*/+), and to WT littermates from each cross. Data was separated by gender and analyzed for significance using a two-tailed Student's t-test with unequal variance and significance at $p < 0.05$. Following sacrifice of animals at six weeks, fat pads were dissected and weighed. The reproductive (epididymal or parametrial) and retroperitoneal/inguinal fat pads on one side of the animal were weighed and compared to the body weight of the individual animals. Fat pads as a percentage of total body weight were analyzed for statistical significance using a two-tailed Student's t-test with unequal variance and significance at $p < 0.05$.

4.6 Histological analysis

At six weeks of age, mice were sacrificed and the following tissues were dissected: brain, pituitary, adrenal, tongue (skeletal muscle), thymus, heart, lung, liver, spleen, kidney, pancreas, small intestine, retroperitoneal/inguinal fat pads, reproductive fat pads, and testis (n=3 of each $Dlk1^{cons}$, $Dlk1^{Ins}$, $Dlk1^{Gh}$, and their corresponding littermate controls). Retroperitoneal/inguinal and reproductive fat pads were also analyzed at 16 weeks of age. Tissues were fixed overnight at 4°C in 4% paraformaldehyde in 1X PBS and processed by the University of Illinois at Urbana-Champaign Veterinary Diagnostic Laboratory. Adipocyte cell area was measured using ImageJ software (Abramoff et al., 2004). Placentae were taken at e12.5, fixed overnight in 4% paraformaldehyde, and sent to Global Path Imaging and Consulting, Ltd. (Metamora, IL, USA) for processing and analysis.

4.7 lacZ expression analysis

Pancreases and pituitaries were dissected from $Dlk1^{Ins}$ and $Dlk1^{Gh}$ mice at six weeks of age and fixed in 4% paraformaldehyde in 1X PBS for 1 hour on ice. Following fixation, tissues were washed in wash buffer (2 mM $MgCl_2$, 0.01% deoxycholic acid, 0.02% NP-40, in PBS) three times for 30 minutes each at RT. β-galactosidase staining was performed in staining solution (1 mg/ml X-gal in DMF, 5 mM potassium ferricyanide, 5 mM potassium ferrocyanide, 2 mM $MgCl_2$, 0.01% deoxycholic acid, 0.02% NP-40, in PBS) overnight in the dark at RT. The next day, tissues were washed in 1X PBS three times, dehydrated in solutions of increasing ethanol concentration, and infused with paraffin wax using a Shandon Citadel 1000 tissue processor (Fisher Scientific, Pittsburgh, PA, USA). Processed tissues were embedded in blocks of paraffin wax using a Shandon Histocentre 2 embedding machine (Fisher Scientific, Pittsburgh, PA, USA). Finally, embedded tissues were cut into 5–10 μm sections using a Leica RM2125 microtome and counterstained using eosin. Coverslips were applied using Permount (Fisher Scientific, Pittsburgh, PA, USA) and images were taken using a Leica MZFLIII dissecting microscope.

4.8 In situ hybridization

Placentae were collected at e12.5 and fixed for 1–2 hours in 4% paraformaldehyde in 1X PBS on ice. Fixative was removed by washing the tissues three times with 1X PBS at RT. The placentae were dehydrated, embedded in paraffin wax, and sectioned as described above for *lacZ* expression. The *Tpbpa* cRNA probe was made using WT e12.5 embryo cDNA as template with the primers: OL1961 – 5′ TCCAAGGACCTCTGAAGAGCTGAA

3′; OL1962 – 5′ AGGAGGCAGTTAATTTGGGAGAGAG 3′. The RT-PCR product was gel isolated and purified using a QIAquick column (Qiagen, Valencia, CA, USA). The purified product was cloned into the pCRII-TOPO vector (Invitrogen, Carlsbad, CA, USA), excised with *Bst*XI, and cloned into the *Sma*I site in the vector pBSIIKS (Agilent Technologies, Santa Clara, CA, USA). *In vitro* transcription reactions using either T7 or T3 RNA polymerase were used to create the digoxigenin-labeled cRNA sense or antisense probes, respectively. *In situ* hybridization was carried out as described previously (Yevtodiyenko and Schmidt, 2006).

4.9 Immunohistochemistry

The following tissues were collected and analyzed using standard immunohistochemical techniques: adult pancreases, adult pituitaries, and e12.5 placentae. Tissues were fixed, dehydrated, paraffin embedded and sectioned as described above in sections 4.7 and 4.8. Heat-induced antigen retrieval (0.3% Sodium Citrate, 0.05% Tween-20, pH 6) was performed followed by washes in 1X PBS. Tissue sections were blocked using 5% donkey normal serum, 1% BSA, 0.5% Tween-20, and 0.75% glycine in 1X PBS for 1 hour at RT. Sections were incubated at 4°C overnight with a 1:50 dilution of rabbit anti-mouse DLK1 primary antibody (sc-25437; Santa Cruz Biotechnology, Santa Cruz, CA, USA). After washing, the sections were incubated in a 1:250 dilution of Alexa Fluor 647-conjugated secondary antibody for 2 hours at RT (Jackson ImmunoResearch Laboratories, West Grove, PA, USA). Sections were rinsed in 1X PBS and DAPI stained (D1306; Life Technologies Corporation, Grand Island, NY, USA). Slides were mounted using Vectashield mounting medium for immunofluorescence (H1000; Vector Laboratories, Burlingame, CA, USA), and imaged on a Zeiss Axiovert 200M microscope.

4.10 Quantitative real-time RT-PCR

Total RNA was extracted from whole adult mouse pituitaries using TRIzol reagent (Invitrogen, Carlsbad, CA, USA), and any DNA contamination was removed by DNase treatment using TURBO DNA-*free* (Ambion, Austin, TX, USA). Reverse transcription was performed with 1 μg of total RNA using Superscript III reverse transcriptase (Invitrogen, Carlsbad, CA, USA). Products of reverse transcription were diluted 1:10, and 2 μl of cDNA was used for subsequent PCR analysis. Control reactions were performed without reverse transcriptase. Quantitative real-time RT-PCR (qRT-PCR) was performed on a DNA Engine Opticon 2 (MJ Research, Hercules, CA) with the following intron-spanning primers: *Gh* (OL1965 – 5′ GATCACTGCTTGGCAATGGCTACA 3′; OL1966 – 5′ TGTAGGCACGCTCGAACTCTTTGT 3′); β-*actin* (OL1112 – 5′ TCTTGGGTATGGAATCCTGTGGCA 3′; OL1113 – 5′ TCTCCTTCTGCATCCTGTCAGCAA 3′). qRT-PCR was performed in triplicate on each sample using SYBR GreenER (Invitrogen, Carlsbad, CA, USA) under the following conditions: uracil DNA glycosylase (UDG) incubation (50°C for 2 minutes); UDG inactivation and DNA polymerase activation (95°C for 10 minutes); followed by 40 cycles of denaturation (94°C for 15 seconds), annealing (62°C for 30 seconds), and elongation (72°C for 15 seconds). A melting curve ranging from 60°C to 95°C was run after each reaction was completed to test for primer dimerization or the formation of multiple products. Relative quantification normalized to *β-actin* was determined using the ΔΔCt method by comparing each sample to the average of all control (*rGH-Cre*/+) samples, with the control average set to 1.

4.11 Fluorescence activated cell sorting

Adult mouse pituitaries (8 each *rGH-Cre*/+ and $Dlk1^{Gh\text{-}pat}$) were dissected and grouped by genotype. Pituitaries were cut into small pieces using surgical blades and incubated in 0.15% trypsin in S-MEM (Spinner's modified Eagle medium) at 37°C with rotating for 3 hours.

Every 45 minutes, the pituitary pieces were passed through a glass Pasteur pipette for 3–5 minutes to further disperse the cells. Fully dispersed cells were pelleted by centrifugation for 5 minutes at 400 × g, resuspended in DMEM (Dulbecco's modified Eagle medium), and cell number and viability was scored using a hemacytometer and Trypan blue. Pituitary cells were cultured in DMEM for 1 hour at 37°C to allow recovery following dissociation. Cells were resuspended in ice cold 10% FBS in PBS supplemented with 100 nM human GRF (Growth hormone releasing factor, National Hormone and Peptide Program, Torrance, CA, USA) to enhance GH at the cell membrane. Aliquots of *rGH-Cre/+* cells were separated for use as "untreated" and "no primary antibody" controls. A 1:1000 dilution of primary antibody (guinea pig anti-rat GH, National Hormone and Peptide Program, Torrance, CA, USA) was added to cells followed by incubation for 1 hour at 4°C in the dark. Cells were washed 3X in ice cold 1X PBS to remove excess primary antibody. Cells were then incubated in 1 μg secondary antibody (goat anti-guinea pig IgG-PE, sc-3732, Santa Cruz Biotechnology, Santa Cruz, CA, USA) in 3% BSA in 1X PBS for 1 hour at 4°C in the dark. Following incubation, cells were washed 3X in 1X PBS, resuspended in 3% BSA, 2 mM EDTA in 1X PBS, and immediately taken for fluorescence activated cell sorting (FACS). FACS was performed by the UIC Flow Cytometry Service using a Beckman Coulter MoFlo cell sorter (Brea, CA, USA). DNA was extracted from sorted cells using standard protocols and PCR was performed across the *Dlk1* deletion region using primers OL657 and OL655 as described in section 4.3 above. DNA sequencing was performed by the UIC DNA Services Facility and confirmed loss of *Dlk1* exons 5 and 6 from $Dlk1^{Gh\text{-}pat}$ somatotrophs.

4.12 Statistical analysis

For determining statistical significance of mouse survival data, a one-tailed Z-test was used. In all other cases, Student's t-test was applied.

Acknowledgments

The authors thank Rhonda Kineman of the University of Illinois at Chicago for the *rGh-Cre* mice and for discussions on the manuscript, Kai Jiao of the University of Alabama for the *Tie1-Cre* mice, Reinhard Faessler for permission to use the *Tie1-Cre* animals, Susan Ball-Kell (Global Path Imaging, Urbana IL) for histology services and interpretation, the National Hormone & Peptide Program and A. F. Parlow for the human GRF and guinea pig anti-rat GH antibodies, and members of the Schmidt laboratory for discussions and review of the manuscript. The $Dlk1^{flox}$ mouse line is available to the research community through The Jackson Laboratory (JAX Stock Number 019074).

References

Abdallah BM, Ding M, Jensen CH, Ditzel N, Flyvbjerg A, Jensen TG, Dagnaes-Hansen F, Gasser JA, Kassem M. Dlk1/FA1 is a novel endocrine regulator of bone and fat mass and its serum level is modulated by growth hormone. Endocrinology. 2007; 148:3111–21. [PubMed: 17446189]

Abdallah BM, Jensen CH, Gutierrez G, Leslie RG, Jensen TG, Kassem M. Regulation of human skeletal stem cells differentiation by Dlk1/Pref-1. J Bone Miner Res. 2004; 19:841–52. [PubMed: 15068508]

Abramoff MD, Magelhaes PJ, Ram SJ. Image Processing with ImageJ. Biophotonics International. 2004; 11:36–42.

Accili D, Drago J, Lee EJ, Johnson MD, Cool MH, Salvatore P, Asico LD, Jose PA, Taylor SI, Westphal H. Early neonatal death in mice homozygous for a null allele of the insulin receptor gene. Nat Genet. 1996; 12:106–9. [PubMed: 8528241]

Amselem S, Duquesnoy P, Attree O, Novelli G, Bousnina S, Postel-Vinay MC, Goossens M. Laron dwarfism and mutations of the growth hormone-receptor gene. N Engl J Med. 1989; 321:989–95. [PubMed: 2779634]

Andersen DC, Jensen L, Schroder HD, Jensen CH. “The preadipocyte factor” DLK1 marks adult mouse adipose tissue residing vascular cells that lack in vitro adipogenic differentiation potential. FEBS Lett. 2009a; 583:2947–53. [PubMed: 19665021]

Andersen DC, Petersson SJ, Jorgensen LH, Bollen P, Jensen PB, Teisner B, Schroeder HD, Jensen CH. Characterization of DLK1+ cells emerging during skeletal muscle remodeling in response to myositis, myopathies, and acute injury. Stem Cells. 2009b; 27:898–908. [PubMed: 19353518]

Ansell PJ, Zhou Y, Schjeide BM, Kerner A, Zhao J, Zhang X, Klibanski A. Regulation of growth hormone expression by Delta-like protein 1 (Dlk1). Mol Cell Endocrinol. 2007; 271:55–63. [PubMed: 17485162]

Anson-Cartwright L, Dawson K, Holmyard D, Fisher SJ, Lazzarini RA, Cross JC. The glial cells missing-1 protein is essential for branching morphogenesis in the chorioallantoic placenta. Nat Genet. 2000; 25:311–4. [PubMed: 10888880]

Armengol J, Villena JA, Hondares E, Carmona MC, Sul HS, Iglesias R, Giralt M, Villarroya F. Pref-1 in brown adipose tissue: specific involvement in brown adipocyte differentiation and regulatory role of C/EBPdelta. Biochem J. 2012 Online ahead of print.

Bachmann E, Krogh TN, Hojrup P, Skjodt K, Teisner B. Mouse fetal antigen 1 (mFA1), the circulating gene product of mdlk, pref-1 and SCP-1: isolation, characterization and biology. J Reprod Fertil. 1996; 107:279–85. [PubMed: 8882295]

Bauer SR, Ruiz-Hidalgo MJ, Rudikoff EK, Goldstein J, Laborda J. Modulated expression of the epidermal growth factor-like homeotic protein dlk influences stromal-cell-pre-B-cell interactions, stromal cell adipogenesis, and pre-B-cell interleukin-7 requirements. Mol Cell Biol. 1998; 18:5247–55. [PubMed: 9710609]

Beamer WG, Sweet HO, Bronson RT, Shire JG, Orth DN, Davisson MT. Adrenocortical dysplasia: a mouse model system for adrenocortical insufficiency. J Endocrinol. 1994; 141:33–43. [PubMed: 8014601]

Bondjers C, He L, Takemoto M, Norlin J, Asker N, Hellstrom M, Lindahl P, Betsholtz C. Microarray analysis of blood microvessels from PDGF-B and PDGF-Rbeta mutant mice identifies novel markers for brain pericytes. Faseb J. 2006; 20:1703–5. [PubMed: 16807374]

Boney CM, Fiedorek FT Jr, Paul SR, Gruppuso PA. Regulation of preadipocyte factor-1 gene expression during 3T3-L1 cell differentiation. Endocrinology. 1996; 137:2923–8. [PubMed: 8770915]

Carlsson C, Tornehave D, Lindberg K, Galante P, Billestrup N, Michelsen B, Larsson LI, Nielsen JH. Growth hormone and prolactin stimulate the expression of rat preadipocyte factor-1/delta-like protein in pancreatic islets: molecular cloning and expression pattern during development and growth of the endocrine pancreas. Endocrinology. 1997; 138:3940–8. [PubMed: 9275085]

Charalambous M, da Rocha ST, Ferguson-Smith AC. Genomic imprinting, growth control and the allocation of nutritional resources: consequences for postnatal life. Curr Opin Endocrinol Diabetes Obes. 2007; 14:3–12. [PubMed: 17940412]

Charalambous M, Ferron SR, da Rocha ST, Murray AJ, Rowland T, Ito M, Schuster-Gossler K, Hernandez A, Ferguson-Smith AC. Imprinted gene dosage is critical for the transition to independent life. Cell Metab. 2012; 15:209–221. [PubMed: 22326222]

da Rocha ST, Charalambous M, Lin SP, Gutteridge I, Ito Y, Gray D, Dean W, Ferguson-Smith AC. Gene dosage effects of the imprinted delta-like homologue 1 (dlk1/pref1) in development: implications for the evolution of imprinting. PLoS Genet. 2009; 5:e1000392. [PubMed: 19247431]

da Rocha ST, Tevendale M, Knowles E, Takada S, Watkins M, Ferguson-Smith AC. Restricted co-expression of Dlk1 and the reciprocally imprinted non-coding RNA, Gtl2: implications for cis-acting control. Dev Biol. 2007; 306:810–23. [PubMed: 17449025]

DeChiara TM, Efstratiadis A, Robertson EJ. A growth-deficiency phenotype in heterozygous mice carrying an insulin-like growth factor II gene disrupted by targeting. Nature. 1990; 345:78–80. [PubMed: 2330056]

DeChiara TM, Robertson EJ, Efstratiadis A. Parental imprinting of the mouse insulin-like growth factor II gene. Cell. 1991; 64:849–59. [PubMed: 1997210]

Duvillie B, Cordonnier N, Deltour L, Dandoy-Dron F, Itier JM, Monthioux E, Jami J, Joshi RL, Bucchini D. Phenotypic alterations in insulin-deficient mutant mice. Proc Natl Acad Sci U S A. 1997; 94:5137–40. [PubMed: 9144203]

Floridon C, Jensen CH, Thorsen P, Nielsen O, Sunde L, Westergaard JG, Thomsen SG, Teisner B. Does fetal antigen 1 (FA1) identify cells with regenerative, endocrine and neuroendocrine potentials? A study of FA1 in embryonic, fetal, and placental tissue and in maternal circulation. Differentiation. 2000; 66:49–59. [PubMed: 10997592]

Gannon M, Shiota C, Postic C, Wright CV, Magnuson M. Analysis of the Cre-mediated recombination driven by rat insulin promoter in embryonic and adult mouse pancreas. Genesis. 2000; 26:139–42. [PubMed: 10686610]

Garces C, Ruiz-Hidalgo MJ, Bonvini E, Goldstein J, Laborda J. Adipocyte differentiation is modulated by secreted delta-like (dlk) variants and requires the expression of membrane-associated dlk. Differentiation. 1999; 64:103–14. [PubMed: 10234807]

Gustafsson E, Brakebusch C, Hietanen K, Fassler R. Tie-1-directed expression of Cre recombinase in endothelial cells of embryoid bodies and transgenic mice. J Cell Sci. 2001; 114:671–6. [PubMed: 11171372]

Hansen LH, Madsen B, Teisner B, Nielsen JH, Billestrup N. Characterization of the inhibitory effect of growth hormone on primary preadipocyte differentiation. Mol Endocrinol. 1998; 12:1140–9. [PubMed: 9717840]

Heikkila M, Peltoketo H, Leppaluoto J, Ilves M, Vuolteenaho O, Vainio S. Wnt-4 deficiency alters mouse adrenal cortex function, reducing aldosterone production. Endocrinology. 2002; 143:4358–65. [PubMed: 12399432]

Hernandez A, Garcia B, Obregon MJ. Gene expression from the imprinted Dio3 locus is associated with cell proliferation of cultured brown adipocytes. Endocrinology. 2007; 148:3968–76. [PubMed: 17510246]

Jensen CH, Krogh TN, Hojrup P, Clausen PP, Skjodt K, Larsson LI, Enghild JJ, Teisner B. Protein structure of fetal antigen 1 (FA1). A novel circulating human epidermal-growth-factor-like protein expressed in neuroendocrine tumors and its relation to the gene products of dlk and pG2. Eur J Biochem. 1994; 225:83–92. [PubMed: 7925474]

Jensen CH, Teisner B, Hojrup P, Rasmussen HB, Madsen OD, Nielsen B, Skjodt K. Studies on the isolation, structural analysis and tissue localization of fetal antigen 1 and its relation to a human adrenal-specific cDNA, pG2. Hum Reprod. 1993; 8:635–41. [PubMed: 8501199]

Joshi RL, Lamothe B, Cordonnier N, Mesbah K, Monthioux E, Jami J, Bucchini D. Targeted disruption of the insulin receptor gene in the mouse results in neonatal lethality. Embo J. 1996; 15:1542–7. [PubMed: 8612577]

Kaneta M, Osawa M, Sudo K, Nakauchi H, Farr AG, Takahama Y. A role for pref-1 and HES-1 in thymocyte development. J Immunol. 2000; 164:256–64. [PubMed: 10605019]

Kingdom J, Huppertz B, Seaward G, Kaufmann P. Development of the placental villous tree and its consequences for fetal growth. Eur J Obstet Gynecol Reprod Biol. 2000; 92:35–43. [PubMed: 10986432]

Kobayashi S, Wagatsuma H, Ono R, Ichikawa H, Yamazaki M, Tashiro H, Aisaka K, Miyoshi N, Kohda T, Ogura A, Ohki M, Kaneko-Ishino T, Ishino F. Mouse Peg9/Dlk1 and human PEG9/DLK1 are paternally expressed imprinted genes closely located to the maternally expressed imprinted genes: mouse Meg3/Gtl2 and human MEG3. Genes Cells. 2000; 5:1029–37. [PubMed: 11168589]

Koni PA, Joshi SK, Temann UA, Olson D, Burkly L, Flavell RA. Conditional vascular cell adhesion molecule 1 deletion in mice: impaired lymphocyte migration to bone marrow. J Exp Med. 2001; 193:741–54. [PubMed: 11257140]

Lakso M, Pichel JG, Gorman JR, Sauer B, Okamoto Y, Lee E, Alt FW, Westphal H. Efficient in vivo manipulation of mouse genomic sequences at the zygote stage. Proc Natl Acad Sci U S A. 1996; 93:5860–5. [PubMed: 8650183]

Larsen JB, Jensen CH, Schroder HD, Teisner B, Bjerre P, Hagen C. Fetal antigen 1 and growth hormone in pituitary somatotroph cells. Lancet. 1996; 347:191. [PubMed: 8544560]

Lee JY, Ristow M, Lin X, White MF, Magnuson MA, Hennighausen L. RIP-Cre revisited, evidence for impairments of pancreatic beta-cell function. J Biol Chem. 2006; 281:2649–53. [PubMed: 16326700]

Lee K, Villena JA, Moon YS, Kim KH, Lee S, Kang C, Sul HS. Inhibition of adipogenesis and development of glucose intolerance by soluble preadipocyte factor-1 (Pref-1). J Clin Invest. 2003; 111:453–61. [PubMed: 12588883]

Li L, Forman SJ, Bhatia R. Expression of DLK1 in hematopoietic cells results in inhibition of differentiation and proliferation. Oncogene. 2005; 24:4472–6. [PubMed: 15806146]

Lupu F, Terwilliger JD, Lee K, Segre GV, Efstratiadis A. Roles of growth hormone and insulin-like growth factor 1 in mouse postnatal growth. Dev Biol. 2001; 229:141–62. [PubMed: 11133160]

Luque RM, Amargo G, Ishii S, Lobe C, Franks R, Kiyokawa H, Kineman RD. Reporter expression, induced by a growth hormone promoter-driven Cre recombinase (rGHp-Cre) transgene, questions the developmental relationship between somatotropes and lactotropes in the adult mouse pituitary gland. Endocrinology. 2007; 148:1946–53. [PubMed: 17289844]

Mei B, Zhao L, Chen L, Sul HS. Only the large soluble form of preadipocyte factor-1 (Pref-1), but not the small soluble and membrane forms, inhibits adipocyte differentiation: role of alternative splicing. Biochem J. 2002; 364:137–44. [PubMed: 11988086]

Moon YS, Smas CM, Lee K, Villena JA, Kim KH, Yun EJ, Sul HS. Mice lacking paternally expressed Pref-1/Dlk1 display growth retardation and accelerated adiposity. Mol Cell Biol. 2002; 22:5585–92. [PubMed: 12101250]

Moore KA, Pytowski B, Witte L, Hicklin D, Lemischka IR. Hematopoietic activity of a stromal cell transmembrane protein containing epidermal growth factor-like repeat motifs. Proc Natl Acad Sci U S A. 1997; 94:4011–6. [PubMed: 9108096]

Nagy A, Moens C, Ivanyi E, Pawling J, Gertsenstein M, Hadjantonakis AK, Pirity M, Rossant J. Dissecting the role of N-myc in development using a single targeting vector to generate a series of alleles. Curr Biol. 1998; 8:661–4. [PubMed: 9635194]

Nueda ML, Baladron V, Sanchez-Solana B, Ballesteros MA, Laborda J. The EGF-like protein dlk1 inhibits notch signaling and potentiates adipogenesis of mesenchymal cells. J Mol Biol. 2007; 367:1281–93. [PubMed: 17320900]

Nueda ML, Garcia-Ramirez JJ, Laborda J, Baladron V. dlk1 specifically interacts with insulin-like growth factor binding protein 1 to modulate adipogenesis of 3T3-L1 cells. J Mol Biol. 2008; 379:428–42. [PubMed: 18466921]

Ohno N, Izawa A, Hattori M, Kageyama R, Sudo T. dlk inhibits stem cell factor-induced colony formation of murine hematopoietic progenitors: Hes-1-independent effect. Stem Cells. 2001; 19:71–9. [PubMed: 11209092]

Postic C, Shiota M, Niswender KD, Jetton TL, Chen Y, Moates JM, Shelton KD, Lindner J, Cherrington AD, Magnuson MA. Dual roles for glucokinase in glucose homeostasis as determined by liver and pancreatic beta cell-specific gene knock-outs using Cre recombinase. J Biol Chem. 1999; 274:305–15. [PubMed: 9867845]

Ross DA, Rao PK, Kadesch T. Dual roles for the Notch target gene Hes-1 in the differentiation of 3T3-L1 preadipocytes. Mol Cell Biol. 2004; 24:3505–13. [PubMed: 15060169]

Sakajiri S, O'Kelly J, Yin D, Miller CW, Hofmann WK, Oshimi K, Shih LY, Kim KH, Sul HS, Jensen CH, Teisner B, Kawamata N, Koeffler HP. Dlk1 in normal and abnormal hematopoiesis. Leukemia. 2005; 19:1404–10. [PubMed: 15959531]

Schmidt JV, Levorse JM, Tilghman SM. Enhancer competition between H19 and Igf2 does not mediate their imprinting. Proc Natl Acad Sci U S A. 1999; 96:9733–8. [PubMed: 10449763]

Schmidt JV, Matteson PG, Jones BK, Guan XJ, Tilghman SM. The Dlk1 and Gtl2 genes are linked and reciprocally imprinted. Genes Dev. 2000; 14:1997–2002. [PubMed: 10950864]

Schuster-Gossler K, Simon-Chazottes D, Guenet JL, Zachgo J, Gossler A. Gtl2lacZ, an insertional mutation on mouse chromosome 12 with parental origin-dependent phenotype. Mamm Genome. 1996; 7:20–4. [PubMed: 8903723]

Sekita Y, Wagatsuma H, Irie M, Kobayashi S, Kohda T, Matsuda J, Yokoyama M, Ogura A, Schuster-Gossler K, Gossler A, Ishino F, Kaneko-Ishino T. Aberrant regulation of imprinted gene expression in Gtl2lacZ mice. Cytogenet Genome Res. 2006; 113:223–9. [PubMed: 16575184]

Smas CM, Chen L, Sul HS. Cleavage of membrane-associated pref-1 generates a soluble inhibitor of adipocyte differentiation. Mol Cell Biol. 1997; 17:977–88. [PubMed: 9001251]

Smas CM, Sul HS. Pref-1, a protein containing EGF-like repeats, inhibits adipocyte differentiation. Cell. 1993; 73:725–34. [PubMed: 8500166]

Soriano P. Generalized lacZ expression with the ROSA26 Cre reporter strain. Nat Genet. 1999; 21:70–1. [PubMed: 9916792]

Steshina EY, Carr MS, Glick EA, Yevtodiyenko A, Appelbe OK, Schmidt JV. Loss of imprinting at the Dlk1-Gtl2 locus caused by insertional mutagenesis in the Gtl2 5′ region. BMC Genet. 2006; 7:44. [PubMed: 17014736]

Takada S, Tevendale M, Baker J, Georgiades P, Campbell E, Freeman T, Johnson MH, Paulsen M, Ferguson-Smith AC. Delta-like and gtl2 are reciprocally expressed, differentially methylated linked imprinted genes on mouse chromosome 12. Curr Biol. 2000; 10:1135–8. [PubMed: 10996796]

Tang Y, Harrington A, Yang X, Friesel RE, Liaw L. The contribution of the Tie2+ lineage to primitive and definitive hematopoietic cells. Genesis. 2010; 48:563–7. [PubMed: 20645309]

Tanimizu N, Nishikawa M, Saito H, Tsujimura T, Miyajima A. Isolation of hepatoblasts based on the expression of Dlk/Pref-1. J Cell Sci. 2003; 116:1775–86. [PubMed: 12665558]

Tornehave D, Jensen CH, Teisner B, Larsson LI. FA1 immunoreactivity in endocrine tumours and during development of the human fetal pancreas; negative correlation with glucagon expression. Histochem Cell Biol. 1996; 106:535–42. [PubMed: 8985741]

Villena JA, Choi CS, Wang Y, Kim S, Hwang YJ, Kim YB, Cline G, Shulman GI, Sul HS. Resistance to high-fat diet-induced obesity but exacerbated insulin resistance in mice overexpressing preadipocyte factor-1 (Pref-1): a new model of partial lipodystrophy. Diabetes. 2008; 57:3258–66. [PubMed: 18835937]

Waddell JN, Zhang P, Wen Y, Gupta SK, Yevtodiyenko A, Schmidt JV, Bidwell CA, Kumar A, Kuang S. Dlk1 is necessary for proper skeletal muscle development and regeneration. PLoS One. 2010; 5:e15055. [PubMed: 21124733]

Wajnrajch MP, Gertner JM, Harbison MD, Chua SC Jr, Leibel RL. Nonsense mutation in the human growth hormone-releasing hormone receptor causes growth failure analogous to the little (lit) mouse. Nat Genet. 1996; 12:88–90. [PubMed: 8528260]

Wang Y, Sul HS. Ectodomain shedding of preadipocyte factor 1 (Pref-1) by tumor necrosis factor alpha converting enzyme (TACE) and inhibition of adipocyte differentiation. Mol Cell Biol. 2006; 26:5421–35. [PubMed: 16809777]

Wolfrum C, Shih DQ, Kuwajima S, Norris AW, Kahn CR, Stoffel M. Role of Foxa-2 in adipocyte metabolism and differentiation. J Clin Invest. 2003; 112:345–56. [PubMed: 12865419]

Yevtodiyenko A, Schmidt JV. Dlk1 expression marks developing endothelium and sites of branching morphogenesis in the mouse embryo and placenta. Dev Dyn. 2006; 235:1115–23. [PubMed: 16456855]

Yevtodiyenko A, Steshina EY, Farner SC, Levorse JM, Schmidt JV. A 178-kb BAC transgene imprints the mouse Gtl2 gene and localizes tissue-specific regulatory elements. Genomics. 2004; 84:277–87. [PubMed: 15233992]

Zhang H, Noohr J, Jensen CH, Petersen RK, Bachmann E, Teisner B, Larsen LK, Mandrup S, Kristiansen K. Insulin-like growth factor-1/insulin bypasses Pref-1/FA1-mediated inhibition of adipocyte differentiation. J Biol Chem. 2003; 278:20906–14. [PubMed: 12651852]

Zhang Y, Shields T, Crenshaw T, Hao Y, Moulton T, Tycko B. Imprinting of human H19: allele-specific CpG methylation, loss of the active allele in Wilms tumor, and potential for somatic allele switching. Am J Hum Genet. 1993; 53:113–24. [PubMed: 8391213]

Zhou Y, Xu BC, Maheshwari HG, He L, Reed M, Lozykowski M, Okada S, Cataldo L, Coschigamo K, Wagner TE, Baumann G, Kopchick JJ. A mammalian model for Laron syndrome produced by targeted disruption of the mouse growth hormone receptor/binding protein gene (the Laron mouse). Proc Natl Acad Sci U S A. 1997; 94:13215–20. [PubMed: 9371826]

- *Dlk1*^{flox} mice were generated to allow conditional deletion of the *Dlk1* gene.
- *Dlk1*^{cons} null mutants display perinatal death and reduced growth of survivors.
- Increased cellularity of *Dlk1*^{cons} placentae may limit maternal-fetal exchange.
- Loss of *Dlk1* in beta cells, somatotropes or endothelial cells causes no pathology.

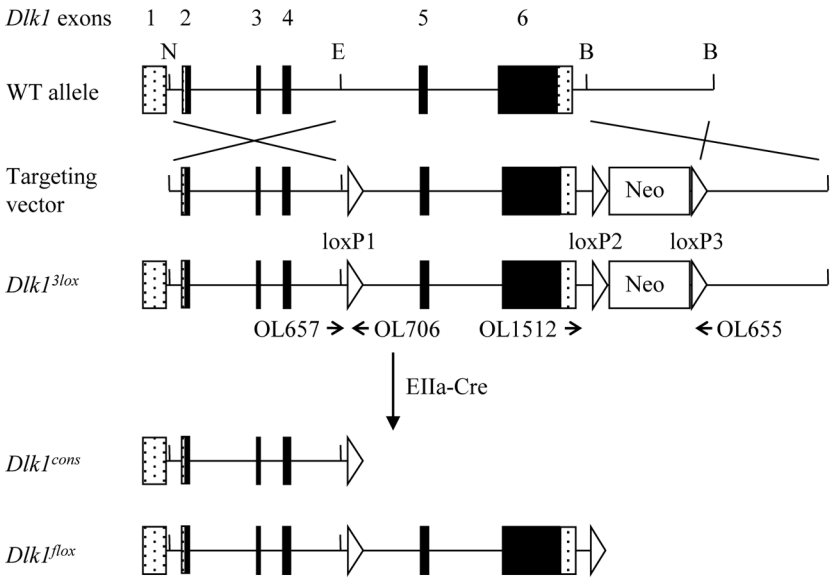

Figure 1.

Schematic of *Dlk1* gene targeting. Protein coding exons of the endogenous *Dlk1* gene are denoted as black boxes and untranslated regions as stippled boxes. N, E, and B represent *Not*I, *Eco*RI, and *Bam*HI restriction sites, respectively. Homologous recombination results in the insertion of three loxP sites (white triangles) and a neomycin cassette (white box), producing the $Dlk1^{3lox}$ allele. $Dlk1^{3lox}$ animals were crossed to *EIIa-Cre* mice to generate $Dlk1^{cons}$ and $Dlk1^{flox}$ mice. $Dlk1^{cons}$ mice lack exons 5 and 6, $Dlk1^{flox}$ mice have loxP sites flanking *Dlk1* exons 5 and 6. The positions of primers used for genotyping assays are shown as arrows and labeled with their corresponding oligonucleotide numbers; the tip of the arrow represents the position of the primer.

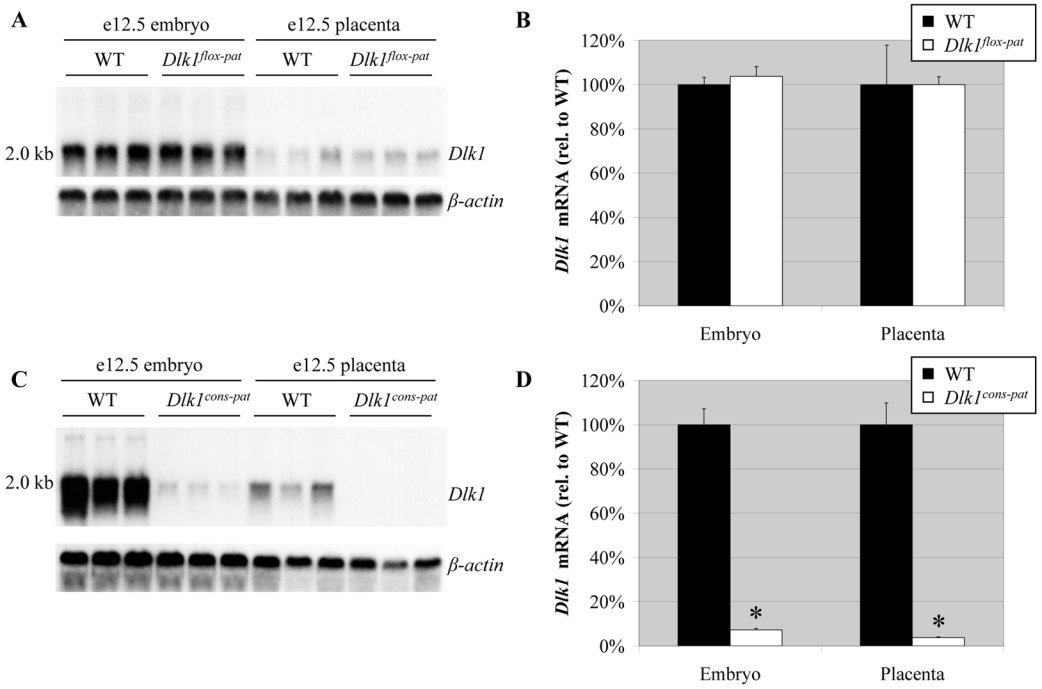

Figure 2.

Dlk1 expression in $Dlk1^{flox}$ and $Dlk1^{cons}$ mice. A) Northern blot of WT and $Dlk1^{flox\text{-}pat}$ embryos and placentae at e12.5. B) Quantification of $Dlk1^{flox\text{-}pat}$ Northern blot. *Dlk1* expression was normalized to *β-actin*, and the WT level was set to 100%. Error bars denote SEM, n = 3 for each genotype. C) Northern blot of WT and $Dlk1^{cons\text{-}pat}$ embryos and placentae at e12.5. D) Quantification of $Dlk1^{cons\text{-}pat}$ Northern blot. *Dlk1* expression was normalized to *β-actin*, and the WT level was set to 100%. Error bars denote SEM, n = 6 for each genotype, * denotes $p < 0.01$.

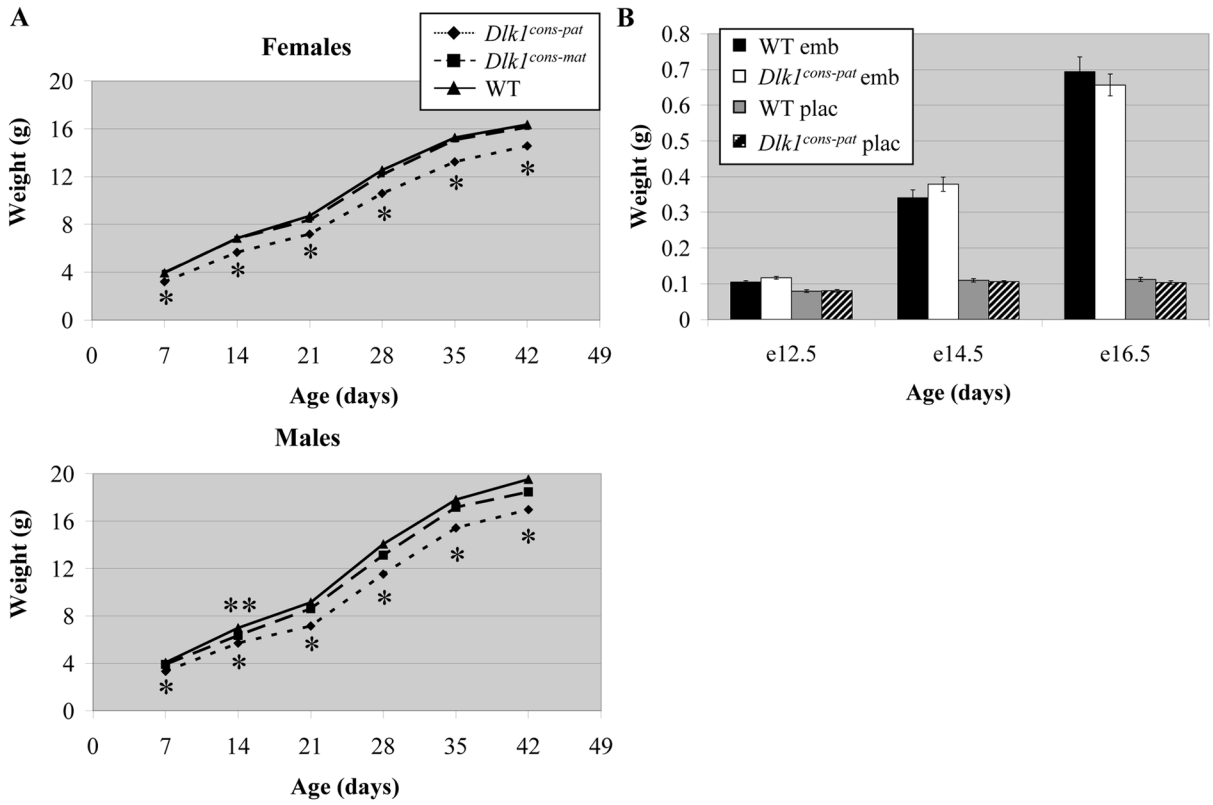

Figure 3.

Growth rates of *Dlk1*$^{cons\text{-}pat}$ mice. A) Weight of female and male WT (solid line, triangles), *Dlk1*$^{cons\text{-}pat}$ (dotted line, diamonds), and *Dlk1*$^{cons\text{-}mat}$ (dashed line, squares) mice from 7 to 42 days of age. n ≥ 13 for each data point. In each panel * denotes $p < 0.01$ for *Dlk1*$^{cons\text{-}pat}$ mice and ** denotes $p < 0.05$ for *Dlk1*$^{cons\text{-}mat}$ mice. B) Weight of WT and *Dlk1*$^{cons\text{-}pat}$ embryos and placentae from e12.5 to e16.5. n ≥ 8 for each data point.

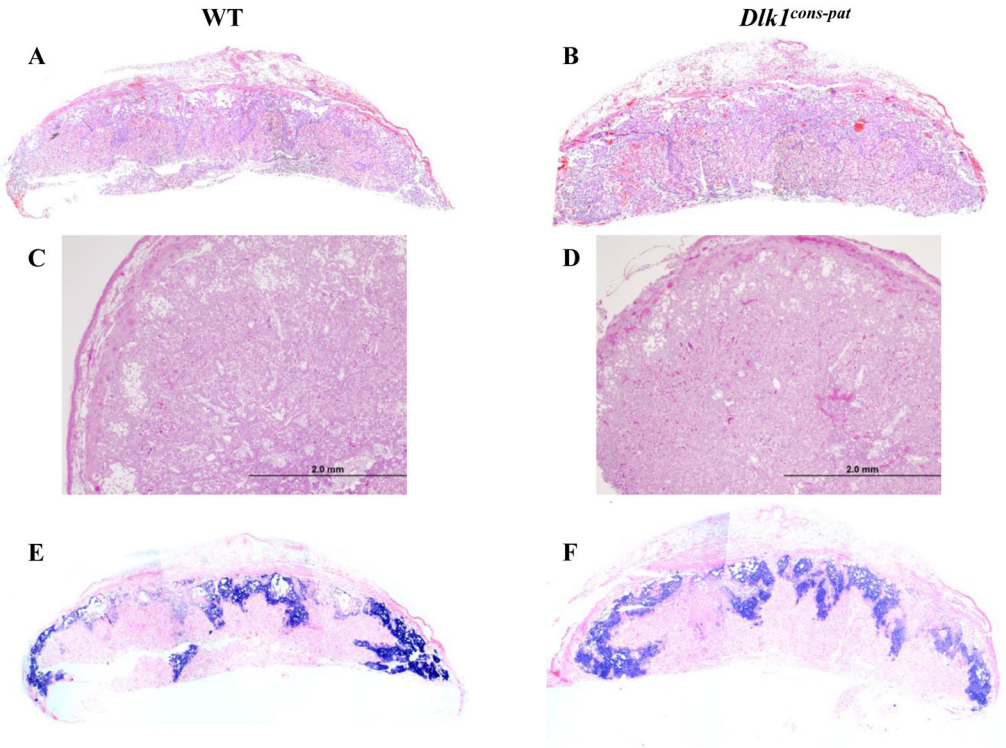

Figure 4.

Histological structure of *Dlk1*$^{cons\text{-}pat}$ placentae. A–D) H & E stained sections of e12.5 WT (A, C) and *Dlk1*$^{cons\text{-}pat}$ (B, D) placentae. Scale bars equal 2.0 mm in C and D. E, F) *Tpbpa in situ* hybridization on e12.5 WT (E) and *Dlk1*$^{cons\text{-}pat}$ (F) placentae.

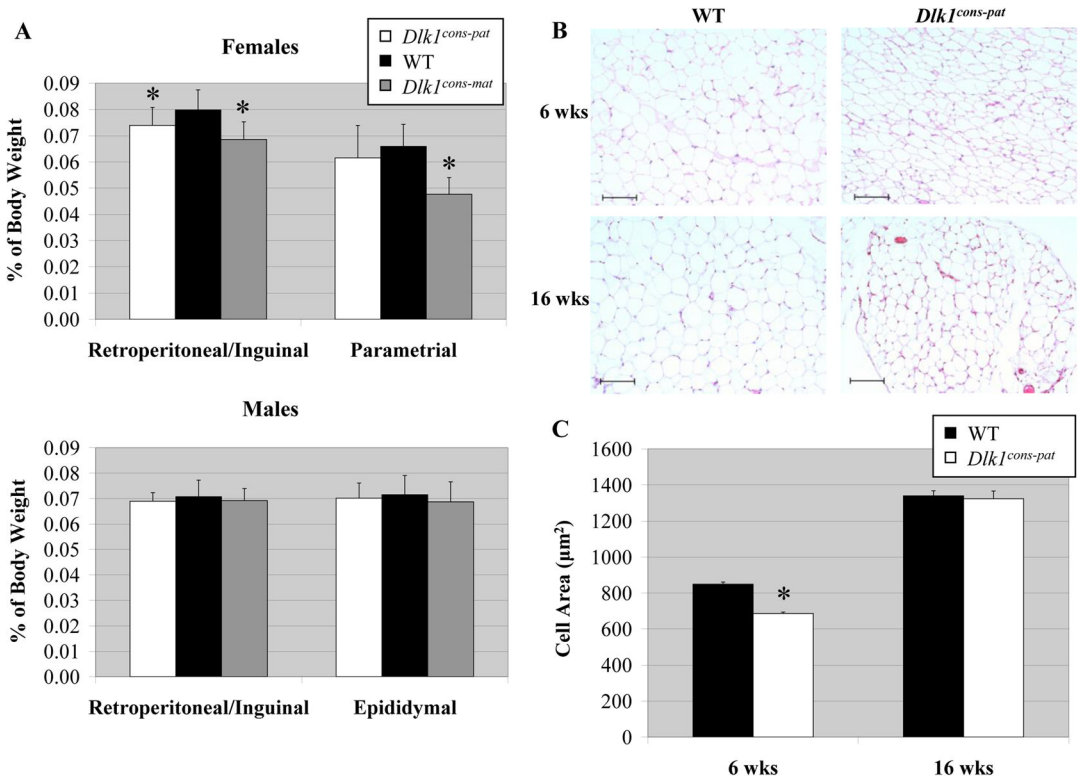

Figure 5.

Fat pad weight and adipocyte morphology of *Dlk1*$^{cons\text{-}pat}$ mice. A) Retroperitoneal/inguinal and reproductive fat pad weights are depicted as a percentage of total body weight in male and female WT, *Dlk1*$^{cons\text{-}pat}$ and *Dlk1*$^{cons\text{-}mat}$ mice. For males n = 20, 8 and 12, and for females n = 20, 14, 4, for WT, *Dlk1*$^{cons\text{-}pat}$ and *Dlk1*$^{cons\text{-}mat}$, respectively. * denotes $p < 0.05$. B) Representative images of H & E stained adipose tissue from 6 and 16 week old WT and *Dlk1*$^{cons\text{-}pat}$ mice. Scale bar = 100 μm. C) Quantification of adipocyte cell area determined using ImageJ software. Two independent images from three animals of each genotype were examined, therefore n = 6 for each genotype. For the six week data, 3,559 and 5,191 cells were measured from WT and *Dlk1*$^{cons\text{-}pat}$ fat pads, respectively. For the sixteen week data, 1,871 and 1,329 cells were measured from WT and *Dlk1*$^{cons\text{-}pat}$ fat pads, respectively. Error bars represent SEM. * denotes p = 2.5E-31.

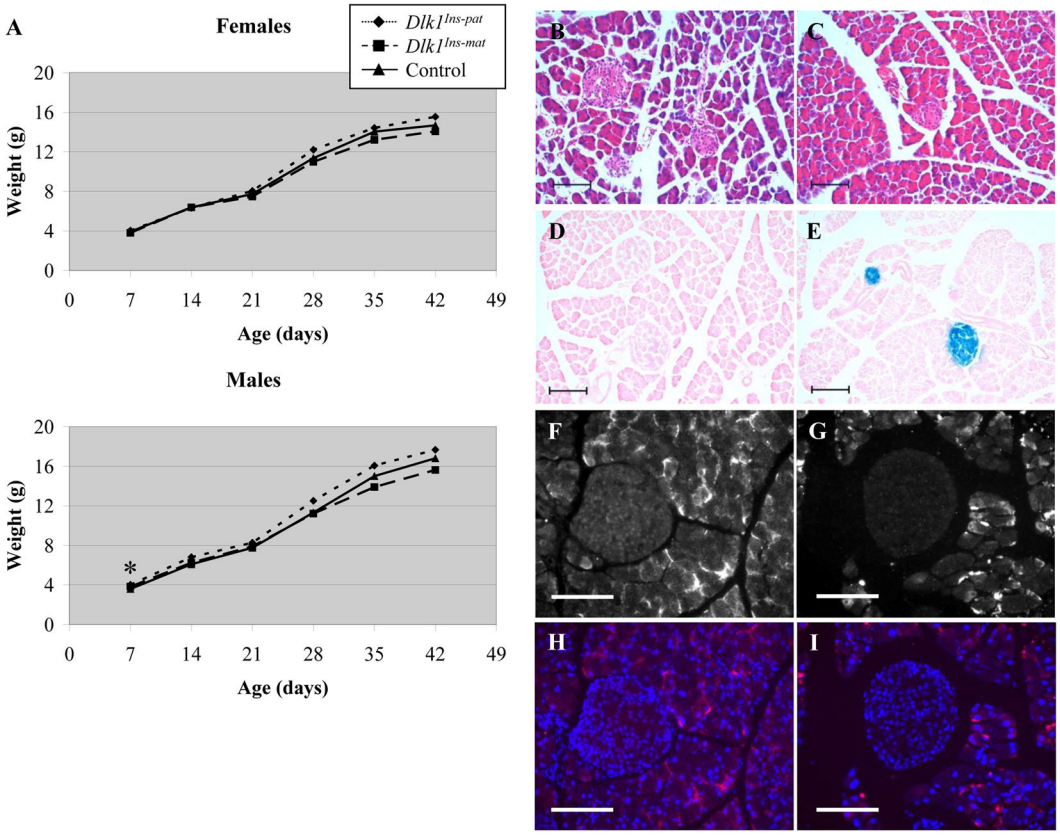

Figure 6.

Growth rates and pancreas morphology of *Dlk1*^{Ins} mice. A) Weight of control (solid line, triangles), *Dlk1*$^{Ins\text{-}pat}$ (dotted line, diamonds), and *Dlk1*$^{Ins\text{-}mat}$ (dashed line, squares) mice from 7 to 42 days of age. n ≥ 19 for each data point. * denotes $p < 0.05$ for *Dlk1*$^{Ins\text{-}pat}$ mice. B, C) H & E stained sections of pancreases from adult control (*rIP-Cre/+*) (B) and *Dlk1*$^{Ins\text{-}pat}$ (C) mice. D, E) β-galactosidase activity in pancreases from adult *ROSA26*/+; +/+ (D) and *ROSA26*/+; +/*rIP-Cre* (E) mice. F-I) Immunohistochemistry using an antibody for DLK1 in adult control (*rIP-Cre/+*) (F, H) and *Dlk1*$^{Ins\text{-}pat}$ pancreases (G, I). Images are shown in black and white for DLK1 alone (F,G) and in color with DLK1 (red) and DAPI (blue) merged (H, I). Scale bars in B–I equal 100 μm.

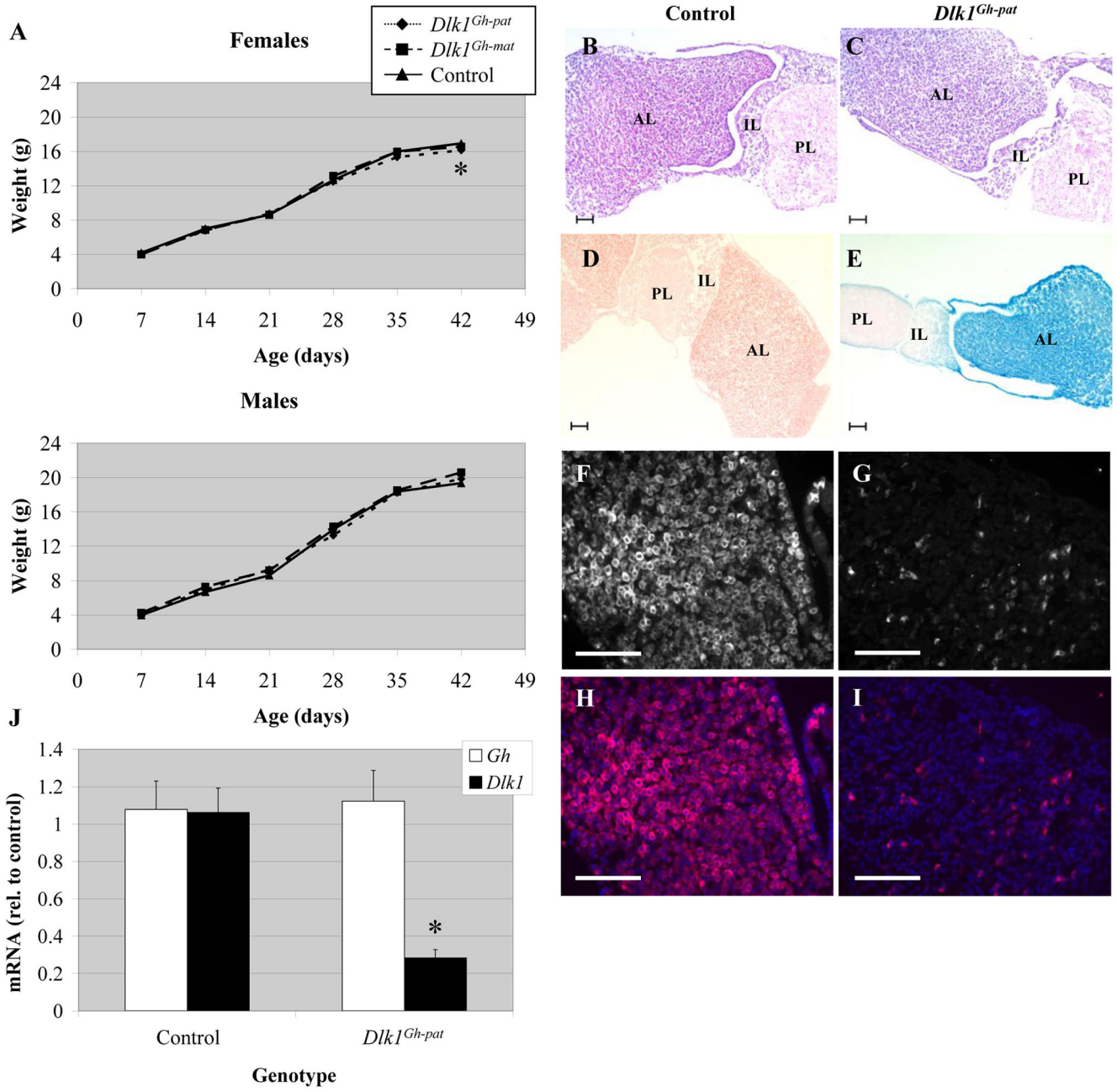

Figure 7.

Growth rates, pituitary morphology and *Gh* expression of *Dlk1*^{Gh} mice. A) Weight of control (solid line, triangles), *Dlk1*$^{Gh\text{-}pat}$ (dotted line, diamonds), and *Dlk1*$^{Gh\text{-}mat}$ (dashed line, squares) mice from 7 to 42 days of age. n ≥ 11 for each data point. * denotes $p < 0.05$ for *Dlk1*$^{Gh\text{-}pat}$ mice. B, C) H & E stained sections of pituitaries from adult control (*rGh-Cre/+*) (B) and *Dlk1*$^{Gh\text{-}pat}$ (C) Mice. D, E) β-galactosidase activity in pituitaries from adult *ROSA26*/+; +/+ (D) and *ROSA26*/+; +/*rGh-Cre* (E) mice. AL indicates anterior lobe, IL, intermediate lobe, and PL, posterior lobe. F-I) Immunohistochemistry using an antibody for DLK1 in adult control (*rGh-Cre/+*) (F, H) and *Dlk1*$^{Gh\text{-}pat}$ anterior pituitaries (G, I). Images are shown in black and white for DLK1 alone (F, G) and in color with DLK1 (red) and DAPI (blue) merged (H, I). Scale bars in B–I equal 100 μm. J) qRT-PCR for *Gh* and *Dlk1*

expression in adult *Dlk1*$^{Gh\text{-}pat}$ pituitaries relative to the average of control values. Error bars represent SEM, * denotes $p < 0.05$.

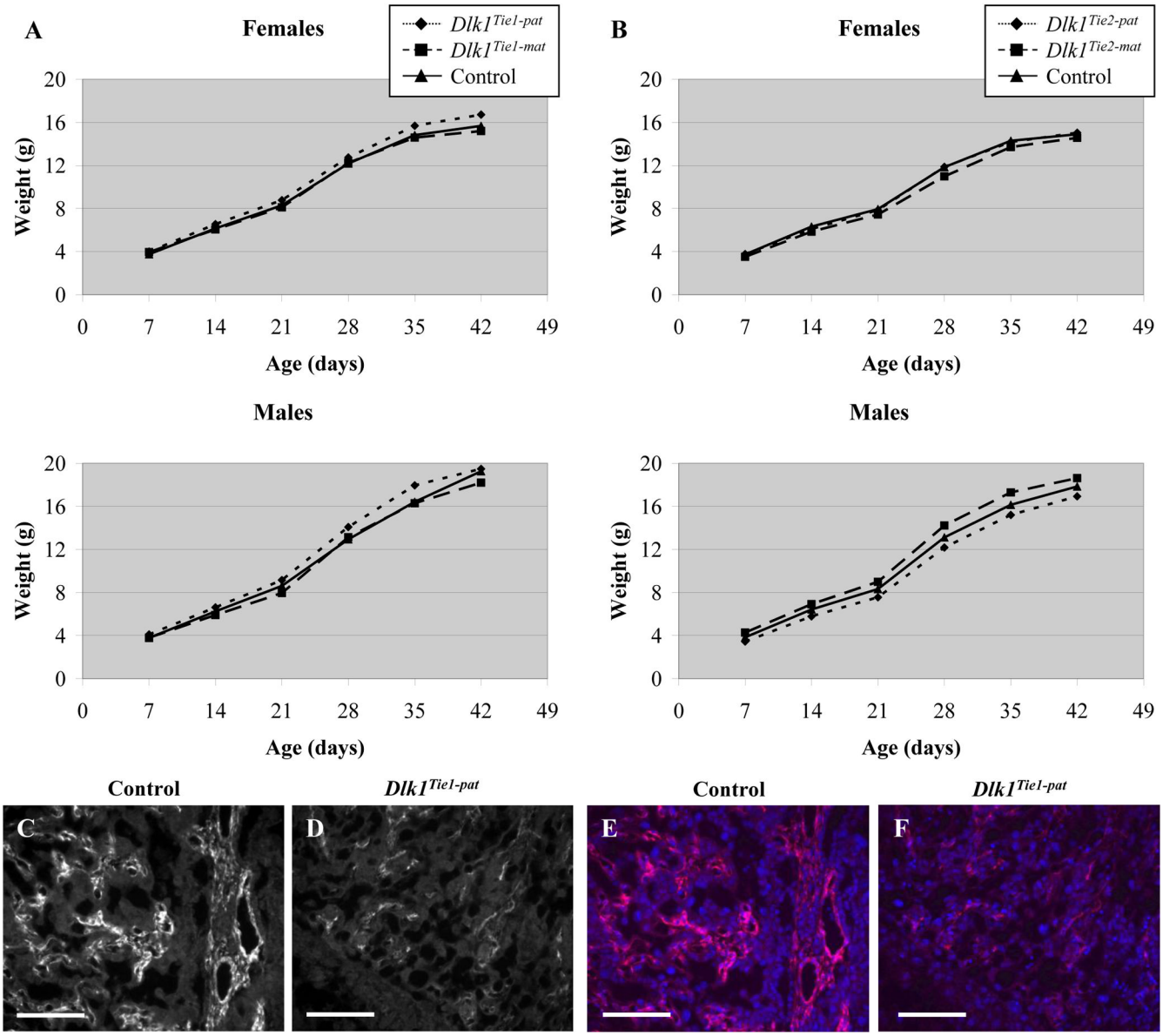

Figure 8.

Growth rates of *Dlk1*^{Tie1} and *Dlk1*^{Tie2} mice. A) Weight of control (*Tie1-Cre/+*) (solid line, triangles), *Dlk1*$^{Tie1\text{-}pat}$ (dotted line, diamonds), and *Dlk1*$^{Tie1\text{-}mat}$ (dashed line, squares) mice from 7 to 42 days of age. n ≥ 9 for each data point. B) Weight of control (*Tie2-Cre/+*) (solid line, triangles), *Dlk1*$^{Tie2\text{-}pat}$ (dotted line, diamonds), and *Dlk1*$^{Tie2\text{-}mat}$ (dashed line, squares) mice from 7 to 42 days of age. n ≥ 4 for each data point. C–F) Immunohistochemistry using an antibody for DLK1 in e12.5 control (*Tie1-Cre/+*) (C, E) and *Dlk1*$^{Tie1\text{-}pat}$ placentae (D, F). Images are shown in black and white for DLK1 alone (C, D) and in color with DLK1 (red) and DAPI (blue) merged (E, F). Scale bars in C-F equal 100 μm.